Supramolecular Coronation of Platinum(II) Complexes by Macrocycles: Structure, Relativistic DFT Calculations, and Biological Effects

Martin Sojka,[†,‡] Jan Chyba,[†,‡] Shib Shankar Paul,[†,‡] Karolina Wawrocka,[†,‡] Kateřina Hönigová,[$] Ben Joseph R. Cuyacot,[†,‡] Abril C. Castro,[§] Tomáš Vaculovič,[‡] Jaromír Marek,[†] Michal Repisky,[Δ] Michal Masařík,[$,£] Jan Novotný,[†,‡] and Radek Marek*[†,‡]

[†] *CEITEC – Central European Institute of Technology, Masaryk University, Kamenice 5, CZ-62500 Brno, Czechia*

[‡] *Department of Chemistry, Faculty of Science, Masaryk University, Kamenice 5, CZ-62500 Brno, Czechia*

[$] *Department of Pathological Physiology, Faculty of Medicine, Masaryk University, Kamenice 5, CZ-62500 Brno, Czechia*

[§] *Hylleraas Centre for Quantum Molecular Sciences, Department of Chemistry, University of Oslo, P.O. Box 1033 Blindern, 0315 Oslo, Norway*

[Δ] *Hylleraas Centre for Quantum Molecular Sciences, Department of Chemistry, UiT – The Arctic University of Norway, 9037 Tromsø, Norway*

[£] *Department of Physiology, Faculty of Medicine, Masaryk University, Kamenice 5, CZ-62500 Brno, Czechia*

***** Email: rmarek@chemi.muni.cz

Abstract

Platinum-based anticancer drugs are actively developed utilizing lipophilic ligands or drug carriers for the efficient penetration of biomembranes, reduction of side effects, and tumor targeting. We report the development of a supramolecular host-guest system built on cationic platinum(II) compounds bearing ligands anchored in the cavity of the macrocyclic host. The host-guest binding and hydrolysis process on the platinum core were investigated in detail by using NMR, MS, X-ray diffraction, and relativistic DFT calculations. The encapsulation process in cucurbit[*7*]uril unequivocally promotes the stability of hydrolyzed dicationic *cis*-$[Pt^{II}(NH_3)_2(H_2O)(NH_2\text{-}R)]^{2+}$ compared to its *trans* isomer. Biological screening on the ovarian cancer lines A2780 and A2780/CP shows time-dependent toxicity. Notably, the reported complex and its β-cyclodextrin (β–CD) assembly achieve the same cellular uptake as cisplatin and cisplatin@β-CD, respectively, while maintaining a significantly lower toxicity profile.

INTRODUCTION

The development of metallodrugs is one of the most active branches of inorganic and bioinorganic chemistry. Many efforts have been devoted to metallocomplexes and organometallics for tumor treatment.[1] Even though the three FDA-approved antitumor compounds (cisplatin, oxaliplatin, and carboplatin)[2] used worldwide show many downsides (e.g., dose-dependent toxicity, acquired and intrinsic resistance of cancer cells, limited solubility),[3] they are the drugs of choice for many types of cancer in combined therapies.[4]

The design of novel platinum-based compounds usually stands on principles of cisplatin chemistry, i.e., the exchange of a chloride ligand followed by presumed binding to nucleic acids. The introduction of new leaving groups or carrier ligands represents a somewhat traditional approach[5] that has led to the second and third generation compounds carboplatin and oxaliplatin. The lower toxicity of carboplatin allows its administration at a higher dosage than that of the parent cisplatin, but its activity is restricted to the same tumor cell lines. In contrast, oxaliplatin shows potential in the treatment of cisplatin-resistant tumors. Both agents, however, must still be administered intravenously.[6] Other Pt-based metallodrugs (e.g., nedaplatin, lobaplatin, heptaplatin) have not been approved worldwide, while more compounds are in various phases of clinical trials.[7]

These described issues fuel the development of novel Pt-based compounds, for which several vital parameters have recently been discussed.[5] The relationship between reactivity and structure mostly holds the key to successful bioactivity. Traditionally, the *cis* arrangement of ligands represents the core of most Pt(II) metallodrugs because it offers more direct binding to biological targets upon aquation. Also, the *cis* isomers are considered kinetically more stable than their *trans* analogues and are therefore favored. However, a range of Pt compounds with *trans* geometry turns out to be highly potent against several cisplatin-resistant cancer cell lines.[8]

The effect of various amines (including amantadine) on anticancer activity was investigated in the early stages of Pt metallodrug development.[9] In many cases, their activity against solid tumors was stated as relatively weak.[10]

The unconventional design of novel Pt-based metallodrugs has split in several directions.[11–16] Some of these lead to multinuclear complexes that exhibit novel modes of action toward cisplatin-resistant cell lines,[17] others focus on more efficient delivery and targeting.[18] Both the efficiency of delivery and the stability of Pt drugs are enhanced by using carrier systems, which provide (to some extent) control over the drug release and reduce side effects.[19,20] Encapsulation within a molecular carrier, such as cyclodextrin (CD) or cucurbituril (CB), may also increase the drug solubility[21] and efficacy.[22,23] Although CD is reported to facilitate the intracellular transport of its guest,[24–26] host-guest complexes with CB cross the cell membranes.[27,28] Two examples of encapsulated Pt complexes are shown in Figure 1.

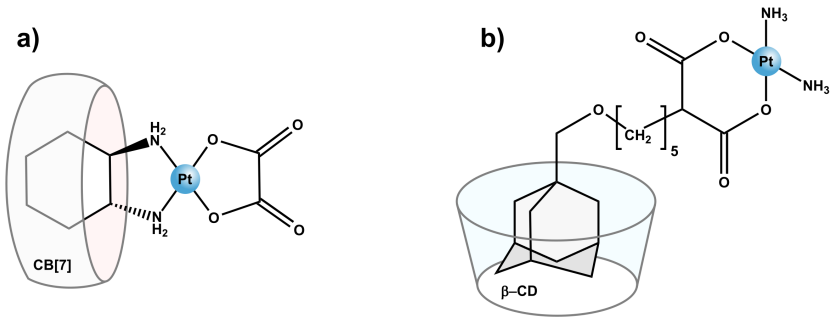

Figure 1. Two examples of supramolecular Pt(II) anticancer agents (a) oxaliplatin in CB7[20] and (b) Pt(II) complex with adamantyl-anchored malonate in *β*-CD.[29]

We contribute to this dynamically developing field of research by synthesizing Pt(II) compounds bearing lipophilic anchors (Figure 2) based on amantadine, rimantadine, and bornylamine–bulky moieties known in medicinal chemistry as exceptional pharmacophores.[30] Nevertheless, their presence in the coordination compounds somewhat reduces their solubility

in an aqueous environment. In this account, we improved their water solubility by forming cationic species and trapping their anchor ligands in the cavity of a macrocyclic carrier – cucurbit[*7*]uril (CB7) or *β*-cyclodextrin (*β*-CD). Our newly introduced ionic Pt(II) compounds feature the possibility of binding to biomolecules such as DNA.

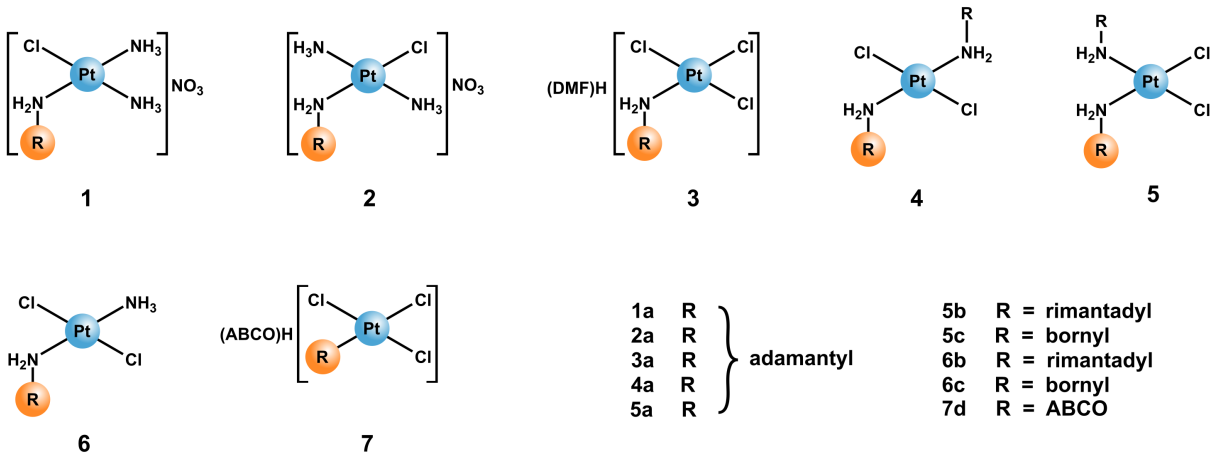

Figure 2. Structure of *cis* and *trans* isomers of square-planar Pt(II) complexes with ammonia, bulky amines, and halogen ligands. (ABCO stands for 1-azabicyclo[2.2.2]octane.)

Following the strategy of supramolecular host-guest design,[31–33] the interactions of our compounds with cavitands have been studied by mass spectrometry (MS), nuclear magnetic resonance (NMR) spectroscopy, and isothermal titration calorimetry (ITC). Among other molecular structures, we are providing a supramolecular assembly with CB7, which expands a limited family of supramolecular metallodrugs.[20,28] We assume that the uptake of our metallodrugs will likely be enhanced by combining the strong hydrophobic effect of bulky cage-hydrocarbon moieties[30,34] with the enhanced permeability and retention effect (EPR)[35] resulting from the increased bulkiness of the supramolecular host-guest assemblies.

RESULTS AND DISCUSSION

Preparation and Characterization of Pt(II) Coordination Compounds

Cisplatin and transplatin, synthesized as described in Lippard's review[36] and references reported therein, were used as reference compounds for biological assessments and as the starting material for the preparation of *cis* and *trans* complexes, Figure 2. The Pt(II) compounds were synthesized starting from cisplatin or transplatin and employing a standard methodology in a two-step substitution process with DMF and amine (Figure 3). For technical details, see Experimental Section.

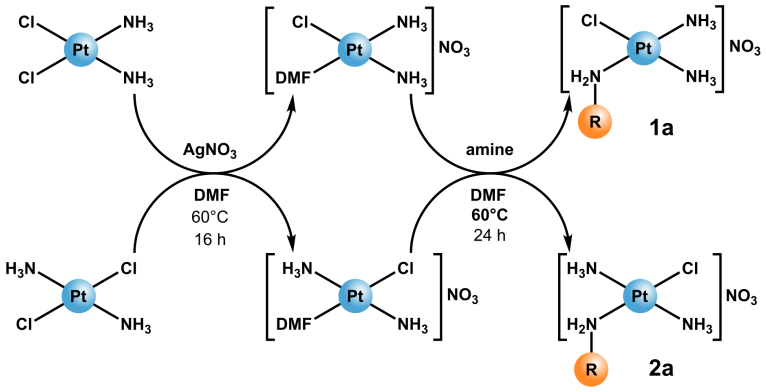

Figure 3. General synthetic approach for preparation of compounds **1a** and **2a**. The other Pt(II) compounds were prepared according to procedures reported elsewhere.[9]

The products were isolated as white to pale yellow solids and characterized by mass spectrometry and NMR spectroscopy (for MS data and ^{195}Pt NMR shifts, see Experimental Section, Tables S1 and S2, and Figure S1 in Supporting Information). Molecular structures of **1a**, **5b**, and **7d** shown in Figure 4 were obtained by X-ray diffraction analysis of crystals grown by slow evaporation of the mother liquor or crystallization from DMF/water solution (for the molecular structure of **5c** and crystal packing, see Figure S2). All determined structures adopt square-planar geometry around the platinum core. The interatomic distances and bond angles

in the coordination polyhedra of the reported compounds vary slightly (see Table S3; cf. **1a** to LEFRUJ,[37] **5b** to DUHKAT,[38] and **7d** to SISWIA[39]).

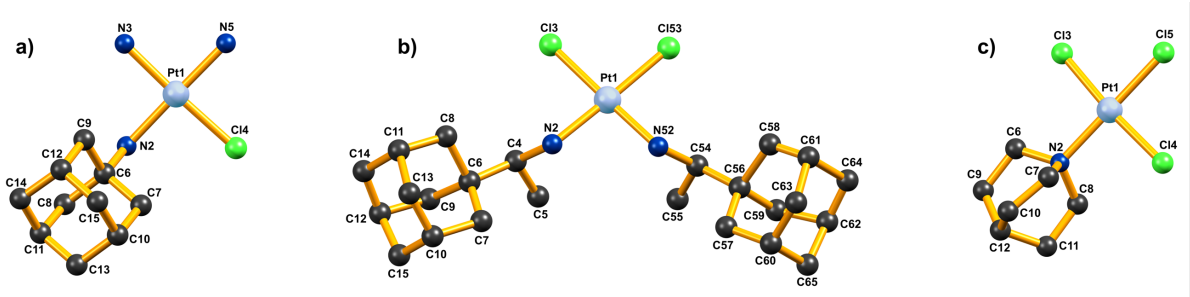

Figure 4. Molecular structure of (a) complex cation of **1a**, (b) compound **5b**, and (c) complex anion of **7d** determined by X-ray diffraction analysis. Counter ions and solvent molecules are omitted for clarity.

Supramolecular Binding of Pt(II) Compounds with *β*-Cyclodextrin and Cucurbit[*7*]uril

Following the strategy of supramolecular metallodrugs, we investigate the host-guest binding between our new Pt(II) compounds and macrocyclic cavitands. Because of the most favorable fit between the adamantyl anchor (180 Å^3)[40] used in our compounds and the internal cavity of *β*-CD (262 Å^3)[41] and CB7 (279 Å^3),[42] these two macrocycles were selected for further investigation. The reported host-guest complexes were prepared in situ by mixing the coordination compound with the macrocycle in H_2O or D_2O. The resulting supramolecular assembly was characterized by mass spectrometry, X-ray diffraction, ITC analysis, and NMR spectroscopy.

Mass Spectrometry

Mass spectra of the host-guest complexes were measured in the positive mode with electron spray ionization. The mass spectrum of the *cis* isomer **1a** with CB7 is dominated by a signal at 780.75 Da, which corresponds to the ion [*cis*-Pt$(NH_3)_2(H_2O)NH_2$-Ad) + CB7]$^{2+}$ with a hydrolyzed cationic part of **1a** (**1a_aq@CB7**), Figure 5a. In contrast, the *trans* isomer **2a** was

determined to be bound with CB7 mainly in a nonhydrolyzed form as a [*trans*-Pt(NH_3)$_2$Cl(NH_2-Ad) + CB7]$^+$ ion at 1578.46 Da or in combination with H^+ or Na^+ cations as charged adducts (charge 2+ or 3+), Figure 5b. These ESI-MS experiments indicate notably different stabilities of the *cis* and *trans* isomers in the presence of the CB7 macrocycle and are investigated in detail in the following sections. The MS data for other complexes are shown in Figure S1.

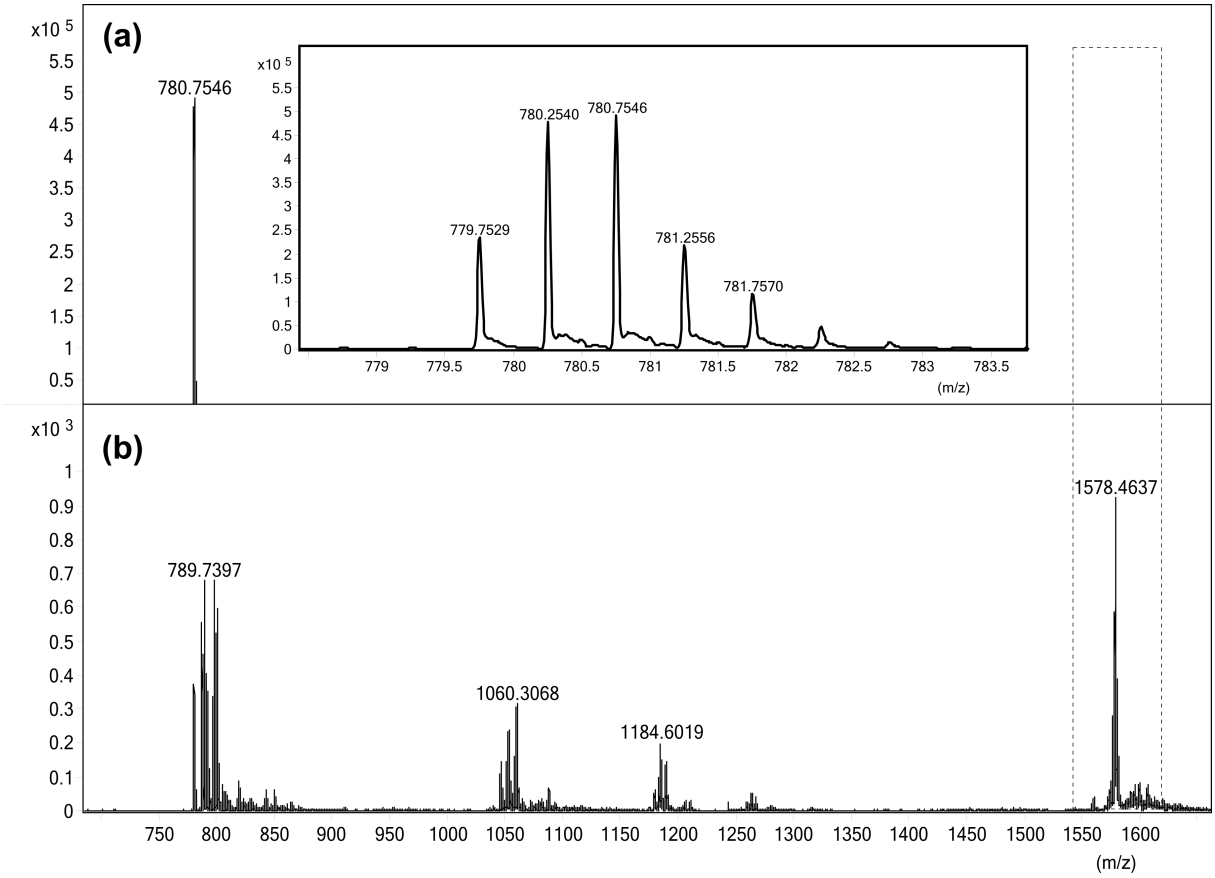

Figure 5. ESI-MS spectra of (a) **1a@CB7** with detailed isotopic pattern and (b) **2a@CB7**. The dashed region highlights the presence of *m*/*z* only for **2a@CB7**, whereas the host-guest assembly **1a@CB7** undergoes ligand substitution of water for chloride–resulting in **1a_aq@CB7**–accompanied by an increase in the molecular charge (1+ → 2+).

X-ray Diffraction

The MS measurement results prompted us to cocrystalize **1a** with CB7. Crystals suitable for single-crystal X-ray diffraction analysis were obtained by crystallizing **1a** from a DMF/water solution. The structure of the host-guest complex **1a@CB7** is shown in Figure 6, the crystal packing in Figure S2c. The adamantyl anchor is trapped in the cavity of CB7 by a hydrophobic effect. However, the N–H groups of the positively charged Pt(II) guest form abundant supramolecular contacts with the partially negatively charged oxygen portal of the CB7 host. Thus, the host-guest complex **1a@CB7** is stabilized not just by hydrophobic forces but also by electrostatic interactions accompanied by electron rearrangement[43,44] and the supramolecular covalency.[45] Note a slight structural deformation which results from the local repulsive interaction between the chloride and the oxygen portal of the CB7, Figure 6. The effects of supramolecular interactions on the host-guest arrangement and stability will be discussed in detail in the following sections.

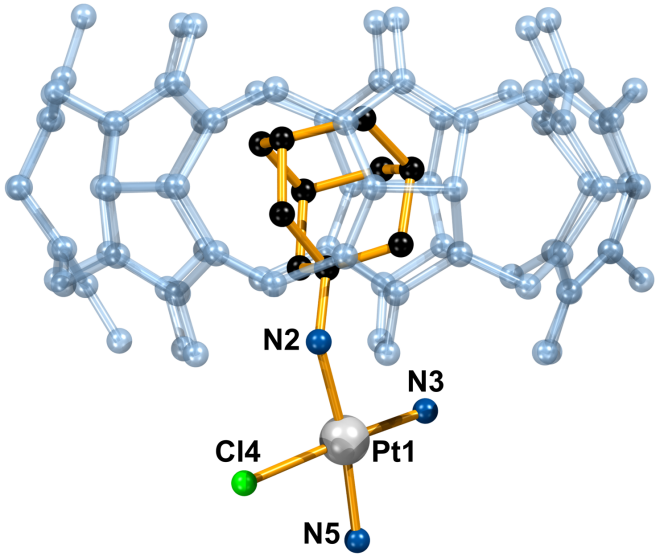

Figure 6. Supramolecular structure of the host-guest complex cation **1a@CB7** as determined by X-ray diffraction analysis. Hydrogens, counterions, and water molecules are omitted for clarity.

Isothermal Titration Calorimetry (ITC)

ITC analysis was used to determine the binding constants and thermodynamic parameters of the host-guest interaction. Because compound **1a** in its binding with CB7 observed by mass spectrometry is rapidly hydrolyzed, we investigated the interaction between compound **2a** (guest) and either the *β*-CD or the CB7 macrocyclic host. The experimental binding constants of **2a** with *β*-CD and CB7 in Milli-Q water at 298 K are shown in Table 1. For additional data (thermodynamic parameters), see Figure S3 and Table S4.

Table 1. Experimental Host-Guest Binding Constants of Compound **2a** with *β*-CD and CB7 Were Obtained by Using Isothermal Titration Calorimetry (ITC)

	binding bonstant (M^{-1})	
Compound	*β*-CD	CB7 [a]
2a	**$(4.69 \pm 0.13) \times 10^4$**	**$(7.26 \pm 0.40) \times 10^{10}$**

[a] Binding analysis was performed with hexamethylenediamine dihydrochloride (HMDA·2HCl) competitor.

As expected, experimentally determined binding constants indicate a significantly higher affinity of compound **2a** for the CB7 cavitand than for *β*-CD. Our results correspond with the binding constants previously obtained for the interaction of organic salts[46] or ruthenium(III) compounds[47,48] bearing an adamantyl anchor with either CB7 or *β*-CD macrocycles.

NMR Spectroscopy

In addition to the experiments discussed above, the supramolecular host-guest interactions between Pt(II) compounds and the macrocycles *β*-CD and CB7 were also investigated by using ^{1}H and ^{195}Pt NMR spectroscopy in D_2O solution.

The interaction between Pt(II) compounds and *β*-CD is relatively weak (see ITC measurements) and the exchange between the free form of the Pt(II) compound and that bound with *β*-CD is quite fast, as indicated by the population-averaged NMR signals. The binding constant of 10^4 M^{-1} extracted from the NMR titration experiments of **1a** and **2a** (Figure S4) corresponds nicely with that calculated for **2a** from the ITC measurements (Table 1). The relative orientation of the host-guest complex with the host protruding from the wider secondary portal of *β*-CD has been confirmed by ROESY experiments (Figure S5).

On the contrary, the interaction of Pt(II) compounds with CB7 results in the formation of strong host-guest complexes. The exchange regime between their bound and free forms is slow, as demonstrated by the resolved NMR lines of the Ad moiety obtained upon the addition of 0.5 equiv of CB7 into the aqueous solution of **1a** (Figure 7).

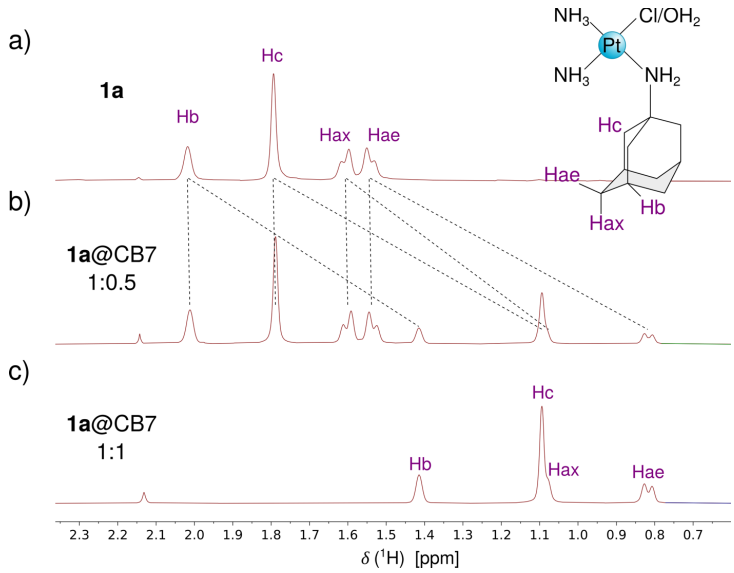

Figure 7. Adamantyl region of the ^{1}H NMR spectra of (a) **1a**, (b) **1a** with 0.5 equiv of CB7, and (c) **1a** with one equivalent of CB7 in D_2O at 298 K. Note that the NMR signals of encapsulated/bound Ad in panels (b) and (c) correspond to the hydrolyzed form of compound **1a** (*vide infra*).

The hydrogen atoms of the adamantane guest are significantly shielded in the presence of CB7 (Figure 7), suggesting that the bulky hydrophobic adamantyl moiety is encapsulated inside the cavity of the macrocycle in the fashion shown by X-ray diffraction (*vide supra*). Moreover, the splitting of the ^{1}H NMR signals corresponding to the CH_2 groups (doublets) of CB7 into two sets of signals (Figure S8) confirms the loss of symmetry of the CB7 host upon encapsulation of the guest molecule.

To investigate the effect of the CB7 host on the platinum coordination sphere in **1a**, we performed parallel measurements of the aqueous solutions of **1a** in D_2O in the absence and presence of CB7 (Figure 8). The hydrolysis of compound **1a** in water is relatively slow, Figure 8a. In contrast, the interaction of **1a** with CB7 promotes the formation of *cis*-$[Pt(NH_3)_2(H_2O)(H_2N\text{-}Ad)]^{2+}$, Figure 8b. Note that the ^{1}H NMR signals of **1a_aq@CB7** appear already in the fresh sample and completely dominate the spectrum after 12 h.

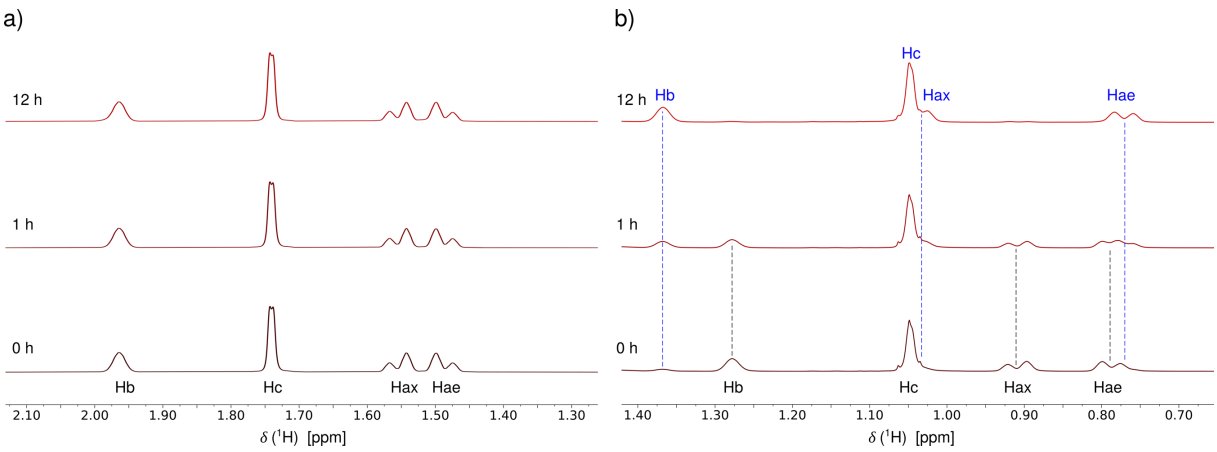

Figure 8. ^{1}H NMR spectra of (a) **1a** and (b) **1a@CB7** measured in D_2O at 293 K in time 0 (bottom), 1 (middle), and 12 (top) hours after the preparation of a fresh sample. The ^{1}H NMR resonances of hydrolyzed **1a_aq@CB7** are marked in blue. For longer experimental times and the effect of KCl (50 mM), see Figures S6 and S7.

Because the suggested hydrolysis at the platinum core can be followed by ^{1}H NMR only indirectly, we performed ^{195}Pt NMR experiments on the extended group of compounds. The ^{195}Pt NMR spectra of the free guest molecule **1a** (–2410 ppm) and its complex with CB7 (–2115 ppm) were recorded under the same conditions in D_2O, Figure 9. However, this large change in ^{195}Pt NMR shift of approximately 300 ppm results from the fast spontaneous aquation that gives **1a_aq@CB7** (cf. ref. 21). A similar chemical shift difference is reported for cisplatin in equilibrium with its aqua-forms (–2160 ppm for *cis*-$[PtCl_2(NH_3)_2]$ and –1854 ppm for *cis*-$[PtCl(NH_3)_2(H_2O)]^+$),[49] and in combination with CB7 (–2109 ppm for *cis*-$[PtCl_2(NH_3)_2]$@CB7 and –1890 ppm for *cis*-$[PtCl(NH_3)_2(H_2O)]^+$@CB7), respectively.[21]

The change in the molecular charge upon aquation, documented by the ^{195}Pt NMR, is considered to be the force driving a shift in the equilibrium toward **1a_aq@CB7**. The stability of **1a_aq@CB7** can be structurally rationalized by a favorable electrostatic interaction between the 2+ charged platinum core and the oxygen portal of CB7 with a partial negative charge, as analyzed in more detail by the DFT calculations, *vide infra*. Thus, the presence of the CB7 host seems to affect both the kinetics and thermodynamics of the aquation process.[50,51]

As shown previously, the platinum aquation process is influenced by the presence of chloride ions.[50] Therefore, we measured the 1:1 mixture of **1a** and CB7 in ~50 mM solution of KCl in D_2O (for ^{1}H NMR spectra, see Figures S7 and S8). The secondary ^{195}Pt NMR shift of only about +20 ppm (the dominant signal in Figure 9d) was clearly observed for **1a@CB7** relative to free **1a**. This demonstrates the large effect of chloride ions in shifting the equilibrium toward the monocationic host-guest complex **1a@CB7**. However, both forms (**1a@CB7** and **1a_aq@CB7**) were simultaneously identified and unequivocally assigned by a ROESY experiment (Figure S9) in the 50 mM KCl solution used.

In contrast to **1a**, hydrolysis of **2a** is not significantly affected by the presence of CB7, and the formation of parent **2a@CB7** was confirmed in an aqueous solution even in the absence of KCl

(cf. Figure 5). This behavior can be rationalized by the limited influence of the trans ligand (Cl or H_2O) on the interactions between **2a** and CB7 and also its effect on the aquation reaction.

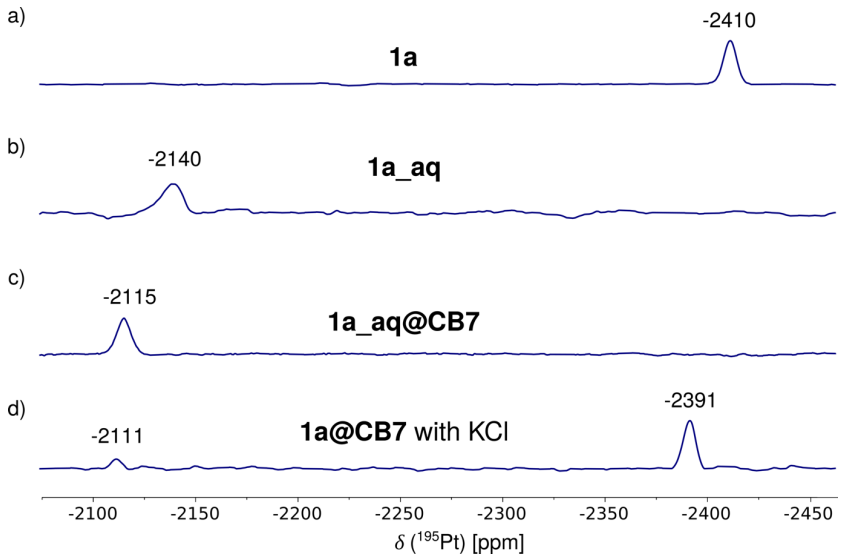

Figure 9. ^{195}Pt NMR spectra of (a) **1a** and (c) **1a_aq@CB7** measured in D_2O at 298 K. (b) The ^{195}Pt NMR spectrum of **1a_aq** synthesized using $AgNO_3$; see Experimental Section. (d) The aquation of **1a** in the presence of CB7 is significantly suppressed in the ~50 mM solution of KCl in D_2O.

Relativistic DFT Calculation of Molecular Structures and NMR Chemical Shifts

To get detailed information about the supramolecular arrangements of host-guest complexes **1a@CB7** and **1a_aq@CB7** and to interpret the NMR experiments, we performed structure optimizations of compounds **1a** and **2a**, their aqua analogues, and their supramolecular host-guest complexes with CB7 by using density functional theory (DFT). In addition, we performed all-electron calculations of ^{195}Pt NMR shifts using the relativistic two-component (2c) zeroth-order regular approximation Hamiltonian (ZORA) as well as the four-component (4c) Dirac-

Coulomb Hamiltonian (DKS), as implemented in the ADF[52] and ReSpect[53] programs, respectively. The results are summarized in Table 2.

Table 2. Experimental [a] and Calculated [b,c] ^{195}Pt NMR Shifts for Compounds **1a** and **2a**, Their Hydrolyzed Forms **1a_aq** and **2a_aq**, and Their Host-Guest Complexes with CB7 in Aqueous Solution[h]

	a	**a_aq**	Δ_{aq}	**a@CB7**	Δ_{CB7}	**a_aq@CB7**	Δ_{aq+CB7} [d]
Experimental [a]							
Compound **1**	-2410	-2140	*+270*	-2391[e]	*+19*	-2115 [f]	**+295**
Compound **2**	-2437	-2177	*+260*	-2415	*+22*	-2173 [g]	**+264**
Calculated, 2c-ZORA/PBE0 [b]							
Compound **1**	-2447	-2157	*+290*	-2503	*-56*	-2155	**+292**
Compound **2**	-2494	-2183	*+311*	-2545	*-51*	-2218	**+276**
Calculated, 4c-DKS/PBE [c]							
Compound **1**	-2312	-1956	*+356*	-2424	*-112*	-2022	**+290**
Compound **2**	-2439	-1980	*+459*	-2466	*-27*	-2062	**+377**

[a] The experimental NMR shifts were referenced using K_2PtCl_4 in D_2O (δ = –1608 ppm) and are reported relative to K_2PtCl_6. [b] The calculated values were obtained with the SO-ZORA(2c)/PBE0/QZ4P/TZ2P/COSMO approach[54,55] as implemented in the program ADF.[52] [c] The calculated values were obtained with the DKS(4c)/PBE/dyall-VTZ/pcS-2/PCM[56–59] approach as implemented in the program ReSpect.[53] The theoretical NMR shifts were referenced[60] to cisplatin, δ = –2139 ppm and are given in ppm. [d] Δ_{aq+CB7} (calculated as $\Delta_{aq+CB7} = \delta_{\mathbf{a\_aq@CB7}} - \delta_{\mathbf{a}}$) does not correspond to the simple sum of Δ_{aq} and Δ_{CB7} due to the structural change of the host-guest complex induced by aquation of the platinum core (see Figure 10). [e] In 50 mM KCl. [f] δ = –2111 ppm in 50 mM KCl (see Figure 9). [g] Compound **2a_aq@CB7** is very unstable in the presence of CB7 contaminated by traces of HCl; therefore, Cl^- was removed from the CB7 solution by using $AgNO_3$ prior to the formation of a host-guest complex. [h] The changes induced by the hydrolysis of chloride ligand (Δ_{aq}) and supramolecular interaction (Δ_{CB7}) are also given. For computational details, see Experimental Section.

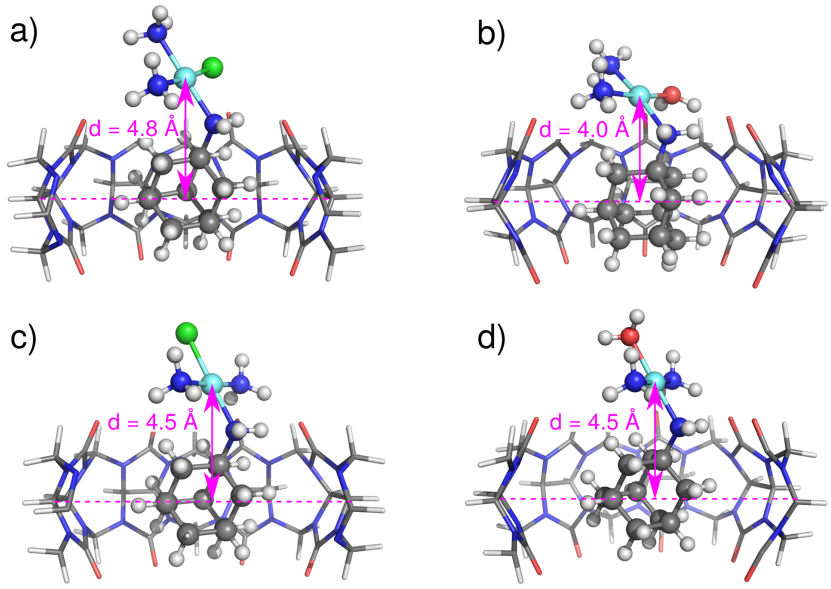

Figure 10. DFT-optimized structures of *cis* (a) **1a@CB7** and (b) **1a_aq@CB7**, and *trans* (c) **2a@CB7** and (d) **2a_aq@CB7**. For Cartesian coordinates, see Supporting Information.

As shown in Table 2, the calculated ^{195}Pt NMR chemical shifts are very sensitive to structural changes induced by both the hydrolysis of the chloride ligand (Δ_{aq}) and the interaction of the guest with CB7 (Δ_{CB7}). Comparison of the theoretical values with the difference between the experimental ^{195}Pt NMR shifts of free **1a** and its CB7-encapsulated form (Δ = +295 ppm) confirms that the encapsulated species corresponds to the hydrolyzed host-guest complex **1a_aq@CB7** (see Table 2). This parallels the observations from the MS analysis. The optimized structures also support our hypothesis that the distance between the $[Pt(N)_3O]^{2+}$ core and the oxygen portal of CB7 is contracted as compared to the parent $[Pt(N)_3Cl]^{1+}$; note the ~0.8 Å shorter vertical distance between the Pt core and CB7 in **1a_aq@CB7**, as indicated in Figure 10. This contraction results from two effects: i) the tilting of the platinum core and ii) the protruding the Ad fragment into the CB7 cavity (~0.6 Å more for **1a_aq@CB7** than for **1a@CB7**). The different position of Ad in CB7 is reflected in the substantial deshielding of the

H_{ax} atoms (see Figure 8b) when comparing the corresponding ^{1}H NMR signals in the hydrolyzed and nonhydrolyzed forms (Table S5).

Following a detailed characterization of the molecular and supramolecular host-guest structures and stabilities of individual compounds in an aqueous solution, we proceed to evaluate their biological activity.

Biological Activity

The cytotoxicity assessment of **1a** and the respective supramolecular assemblies with *β*-CD and CB7 was performed using two cell lines, A2780 (an ovarian cancer cell line) and A2780/CP (a cisplatin-resistant ovarian cancer cell line). The rest of the reported compounds were either poorly soluble or precipitated out of the media, making their evaluation impossible.

The assessment was set for two different times (24 and 48 h) to observe the time-dependent cytotoxicity of the compounds using reference cisplatin as a gold standard. Compound **1a** was utterly soluble in the culture media used with no remnants visible under the microscope; no residues were visible after combining **1a** with the respective macrocycles. In general, compound **1a** evinces concentration-dependent cytotoxicity (see Figure 11 and Table S7), being more toxic to the A2780 cell line. Notably, the cytotoxicity of **1a** and the respective supramolecular assembly **1a@*β*-CD** become more pronounced after 48 h for both cell lines.

The encapsulation of cisplatin in either of the two macrocycles shows a marginal effect on the cytotoxicity of the drug, which can be related to the structure of cisplatin and the relatively weak host-guest binding constants ($530 \pm 30\ M^{-1}$ for CB7[20] and an assumably small value for *β*-CD[61]). In contrast, the formation of supramolecular assemblies of **1a** with *β*-CD or CB7 results in a decrease in cytotoxicity (cf. binding constants in Table 1). As expected, this effect is more pronounced for the stronger supramolecular complex **1a@CB7** (or more probably

1a_aq@CB7) compared to **1a@*β*-CD** (Figure 11 and Table S7). In a very simplified view, this can be imagined as a hindered release from CB7 because of the affinity between the host and guest.[22] Note that the absolute binding affinity is not always the relevant parameter for estimating the biological response, which can also be significantly influenced by the kinetics of the release.[28,62] However, our NMR and ITC experiments (*vide supra*) consistently show significantly higher affinity and slower exchange between the free and bound forms of CB7 as compared to *β*-CD.

Although the encapsulation often ends with a decreasing cytotoxicity,[63] it also protects the guest metallodrug against rapid degradation.[20,64] Also, as demonstrated recently,[19] introducing a bulky adamantyl group (and *β*-CD) to the Pt(II) complex can reduce the cytotoxicity profile *in vitro*, but the compound can simultaneously exhibit markedly high efficacy *in vivo*.

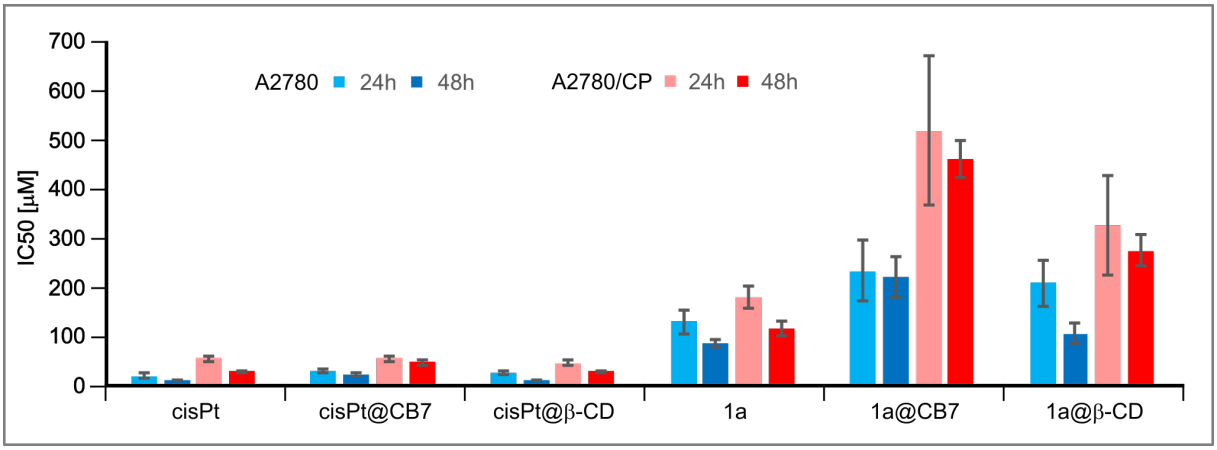

Figure 11. Cytotoxicity (IC50 in µM) of **1a**, **1a@CB7**, **1a@*β*-CD**, cisplatin (cisPt), and respective supramolecular cisplatin assemblies to cisplatin-sensitive A2780 (blue) and cisplatin-resistant A2780/CP (red) cell lines observed after 24 (light) and 48 (dark) hours.

To further explore aspects of the increased cytotoxicity of the compounds observed after 48 h treatment, the platinum uptake was determined using a sub-IC50 concentration of cisplatin (3.5

μM) for all compounds and host-guest complexes. The treated cell samples were analyzed by ICP-MS to determine nanograms of Pt per 10^9 cells (Figure 12). Generally, the Pt content increases with the treatment time for free **1a** and also for supramolecular assemblies (see blue lines of A2780 in Figure 12). Note that the decrease in cisplatin uptake can be assigned to various factors, including the altered activity of transport proteins, cisplatin efflux, or apoptosis.[65–67] While the encapsulation of **1a** by the *β*-CD initially shows no significant impact on the platinum uptake (likely due to the relatively weak binding of **1a** to *β*-CD, *vide supra*), CB7 significantly suppresses the transition of **1a** (or **1a_aq**) into cells *in vitro*. Although some reports suggest improved uptake of platinum metallodrug upon the formation of a supra-/macromolecular assembly,[23,68,69] we draw a more pressing conclusion from the obtained results. Platinum uptake is comparable for the tested compounds on the respective cell lines and experimental times; thus, it depends rather weakly on the molecular structure. In contrast, **1a** and **1a@*β*-CD** show significantly lower toxicity at an uptake comparable to that of cisplatin (cf. Figure 11). This observation calls for further systematic study with great potential for identifying a novel chemical strategy.

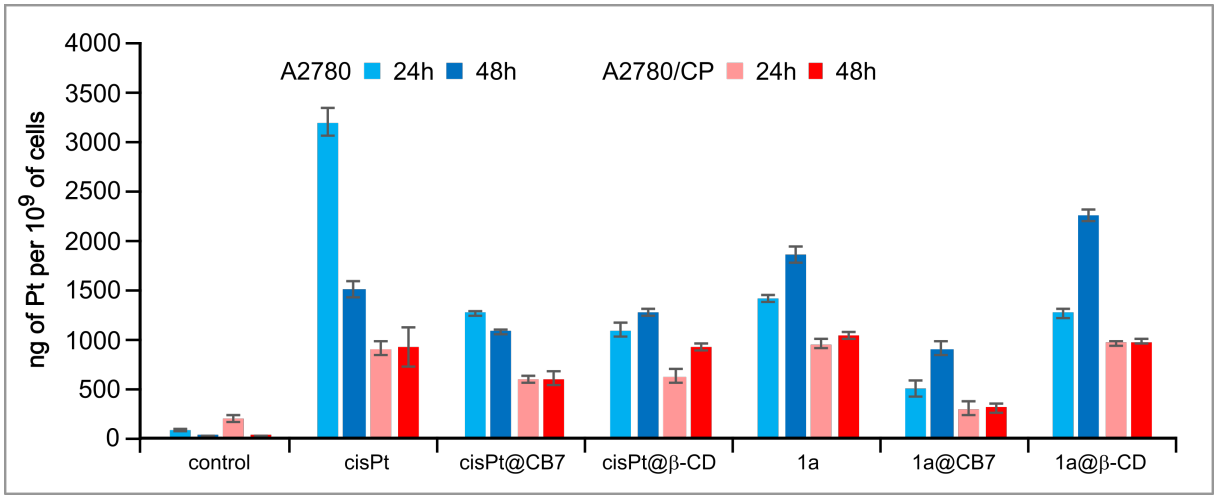

Figure 12. Platinum content in nanograms per 10^9 cells. The reported compounds **1a**, **1a@CB7**, and **1a@*β*-CD** are compared to reference cisplatin (cisPt) and its respective supramolecular

complexes observed on cisplatin-sensitive A2780 (blue) and cisplatin-resistant A2780/CP (red) cancer cell lines after 24 (light) and 48 (dark) hours of treatment.

CONCLUSION AND PERSPECTIVES

In this study, we optimized the synthesis of Pt(II) cationic, neutral, and anionic complexes with bulky amines. We found that the cationic complexes are the most favorable for host-guest binding with macrocycles (particularly with cucurbiturils) while showing promising antiproliferative activity.

The structures of the reported compounds were determined unequivocally by using NMR spectroscopy, mass spectrometry, X-ray diffraction, and theoretical calculations. We monitored the stability of these compounds in aqueous solutions by ^{1}H and ^{195}Pt NMR spectroscopy and mass spectrometry. The process of aquation of the *cis* derivative of **1a** is enhanced in the presence of CB7. This aquation step can be considered as the metallodrug activation, although the strong binding of the activated double-charged form prevents its fast release from the cavity of the CB7. The observed structural changes were manifested in the ^{195}Pt NMR spectra and interpreted in detail utilizing relativistic DFT calculations.

Compound **1a** and its respective supramolecular assemblies were evaluated for biological activity using two cell lines, A2780 and cisplatin-resistant A2780/CP. The IC50 values were determined after 24 and 48 h, showing the concentration-dependent toxicity of the compounds. The toxicity observed for **1a** was lower overall (larger IC50) than that for cisplatin. As reports on amantadine-modified Pt drugs indicate possibilities for further development,[70,30,71] our next step aims to evaluate the reported compounds on a wider cell panel profile.

The platinum uptake was assessed after 24 and 48 h to investigate the penetration of the compounds into the cells. Notably, the combination of **1a** with the β-CD macrocycle exceeds

the uptake values of cisplatin by 50 % after 48 h of treatment while being less toxic. The observed slow onset of action combined with promoted cellular uptake opens up the future for the increased efficacy in single-dose *in vivo* experiments. In that regard, the small molecule could benefit from being protected by the carrier against fast systemic clearance, while simultaneously requiring a smaller overall dose.

Our observations for the CB7 carrier are different from those for *β*-CD. The strong host-guest complex prevents effective release of the activated drug (aquated form **1a_aq**) from the CB7 carrier and reduces the biological response. In order to improve the release of the platinum compound, an anchor moiety at the Pt core with somewhat lower affinity for the carrier should be used, or the stability of the linker between the supramolecular anchor and the Pt core should be modified by inserting a labile chemical bond such as ester or amide. This could lead to more efficient release of the drug while preserving the transport benefits of the macrocycle. Investigations following the above two strategies are underway in our laboratory.

EXPERIMENTAL SECTION

Methods

IR and Raman Spectroscopy and Mass Spectrometry. IR spectra were obtained on an FT-IR Bruker ATR spectrometer. Raman IR spectra were recorded on a HORIBA LabRAM microspectrometer using laser excitations of 532 and 785 nm. Electrospray ionization mass spectrometry (ESI-MS) measurements were acquired on an Agilent 6224 Accurate-Mass TOF LC-MS.

Isothermal Titration Calorimetry. ITC analysis was performed using an automated isothermal microcalorimeter (Malvern AutoITC200). The samples were dissolved in Milli-Q water, and the ITC measurements were carried out at 298 K using a stirring speed of 750 rpm. After an

initial delay of 120 s, 40 injections (2.0 μL each) of the solution were added from a microsyringe to the solution in the cell with time spacing 300 s. Titrations were performed in triplicate, and blank measurements were realized to determine and subtract the heat effect accompanying the dilution of components during the ITC experiment. The raw experimental data were analyzed using MicroCal PEAQ-ITC software. The data were fitted to a theoretical titration curve using a model with a single binding site, *vide infra*.

NMR Spectroscopy. ^{1}H, ^{13}C, and ^{195}Pt NMR spectra were recorded on Bruker Avance III HD 700 MHz, Bruker Avance III HD 600 MHz, and Bruker AVANCE III TM 500 MHz spectrometers at 298.2 K (unless specified otherwise). ^{1}H and ^{13}C NMR spectra were referenced internally to residual solvent peaks, and chemical shifts are reported relative to tetramethylsilane, TMS (δ = 0 ppm). The ^{195}Pt spectra were recorded in DMF-d_7, D_2O, or $CDCl_3$ for locking purposes and referenced to K_2PtCl_6.

Dipolar interactions between individual components of the inclusion complexes were detected by using 2D ^{1}H-^{1}H ROESY experiments[72] with presaturation of the residual HDO signal (spin-lock time 75-150 ms). Correlation signals were assigned using the program NMRFAM-Sparky.[73] Overlapping ^{1}H signals were resolved using ^{1}H-^{13}C HSQC (^{1}J = 130 Hz).[74]

Single-Crystal X-ray Diffraction. Diffraction data were collected on a Rigaku MicroMax-007 HF rotating anode CCD diffractometer. The structures were solved by direct methods and refined by full matrix least-squares methods using the ShelXT[75] and SHELXL[76] software packages. The PLATON SQUEEZE[77] was used to reduce a heavily disordered solvent contribution from the structure factor calculations for **1a@CB7**. Crystal data and structure refinement parameters are listed in Table 3.

Table 3. Selected Crystallographic Data for Compounds **1a**, **5b**, **5c**, and **7d** and the Supramolecular Complex **1a@CB7**.

	1a	5b	5c	1a@CB7	7d
CCDC no	2100921	2100922	2100923	2100928	2100924
chemical formula	$C_{10}H_{23.50}Cl_2N_3O_{0.25}Pt$	$C_{24}H_{44}Cl_2N_2PtO$	$C_{23}H_{45}Cl_2N_3OPt$	$C_{52}H_{65}ClN_{31}O_{14}Pt$	$C_{14}H_{27}Cl_3N_2Pt$
formula weight	455.81	642.60	645.61	1578.89	524.81
crystal system	triclinic	monoclinic	triclinic	monoclinic	triclinic
space group	*P*-1	*C 2/c*	*P*-1	*P*2-1/*n*	*P*-1
a (Å)	12.7412(2)	62.952(3)	10.4323(3)	23.3466(2)	6.7178(1)
b (Å)	13.7356(2)	13.4476(5)	11.2998(3)	23.3775(2)	10.1416(2)
c (Å)	18.5570(3)	11.9906(5)	13.3670(4)	30.8826(4)	12.7994(2)
α (deg)	73.312(2)	90	76.965(2)	90	92.7280(1)
β (deg)	79.207(1)	98.068(3)	69.102(2)	103.838(1)	101.3480(1)
γ (deg)	89.766(1)	90	65.578(3)	90	91.3110(1)
V (Å^3)	3051.55(9)	10050.2(7)	1334.71(7)	16366.1(3)	853.53(3)
Z	8	8	2	8	2
$D_{calcd.}$ (g cm^{-3})	1.984	0.849	1.606	1.282	2.042
μ (mm^{-1})	9.53	2.91	5.48	1.82	8.68
measured/unique reflections	26864/11561	23129/8628	15403/4974	204456/28796	8676/3242
data/parameters/restraints	11561/600/4	8628/274/263	4974/467/1260	28796/1836/2040	3242/3126/184
R_1/wR_2 [I > 2σ(I)]	0.0396/0.1081	0.0749/0.2007	0.0222/0.0510	0.0618/0.1677	0.0158/0.0358
R_1/wR_2 [all data]	0.0405/0.1090	0.0944/0.2170	0.0228/0.0511	0.0652/0.1700	0.0166/0.0365
GOF	1.034	0.970	1.271	1.035	1.041
$\Delta\rho_{max}/\Delta\rho_{min}$ (e Å^{-3})	6.12/−2.71	2.13/−7.76	0.82/−0.80	2.49/−1.54	1.22/−0.71

Quantum Chemical Calculations

Structure Optimization. All electronic-structure calculations were performed at the density-functional theory (DFT) level. Equilibrium geometries were computed with the Amsterdam Density Functional (ADF, ver. 2019) program,[52] using the dispersion-corrected PBE-D3-BJ[78,79] functional in conjunction with uncontracted Slater-type orbitals (STOs) of triple-ζ quality plus one set of polarization functions (TZ2P).[80] Spin-orbit (SO) relativistic corrections were included within the zeroth-order regular approximation Hamiltonian (ZORA),[54,55,81,82] and the conductor-like screening model (COSMO)[83–85] was used to simulate bulk solvation in water.

Relativistic Calculations of NMR Chemical Shifts.[86,87] *Two-Component ZORA Approach*. The ^{1}H and ^{195}Pt NMR shielding constants were calculated with the ADF program (ver. 2017)[52] using the 2c-ZORA Hamiltonian at the PBE0[88]/TZ2P[80] level in COSMO[83,85] (solvation radius 1.93 Å, dielectric constant 78.4). The ^{195}Pt NMR chemical shifts were calculated relative to cisplatin (a secondary reference with δ = –2139 ppm),[60] and are reported relative to $[PtCl_6]^{2-}$.

Four-Component Dirac-Kohn-Sham Approach. The ^{195}Pt NMR shifts were calculated by using a full four-component Dirac-Kohn-Sham (DKS) approach in combination with the Dirac-Coulomb Hamiltonian as implemented in the ReSpect program (ver. 5.1).[53] The PBE exchange-correlation functional was selected, and the polarizable continuum model (PCM)[58] was included to simulate water solvent. Mixed uncontracted basis sets for large-component were employed to preserve high accuracy at a lower computational cost, combining the Dyall's VTZ[89–91] basis set for platinum, the Jensen's pcS-2[92,93] for the nearest substituents around Pt (i.e., Cl, H_2O, NH_2, and NH_3) and the IGLO-II[94] basis set for the remaining light atoms (adamantyl and CB7 macrocycle). The corresponding small-component basis was generated according to the restricted kinetic balance (RKB) condition[95] and the restricted magnetic balance (RMB) condition.[57,56] The gauge-origin dependence was handled using gauge-including atomic orbitals (GIAOs).[57,96] In order to accelerate the calculations, the relativistic electron repulsion integrals and related two-electron Fock contributions were calculated using the resolution-of-identity for the two-electron Coulomb term,[59] which has demonstrated good accuracy for large systems while reducing the computational cost.[56,96,97] The ^{195}Pt NMR shifts were referenced relative to cisplatin as the secondary reference (see the 2c approach above).

Chemical Synthesis

Chemicals. Potassium tetrachloroplatinate, adamantylamine, bornylamine, rimantadine hydrochloride, and solvents were purchased from Sigma-Aldrich Co. and Alfa Aesar. *cis*-$PtCl_2(NH_3)_2$ and *trans*-$PtCl_2(NH_3)_2$ were prepared according to the method reported by Dhara.[101] Rimantadine was prepared from rimantadine hydrochloride as the starting material. Solvents were used as received without drying or purification.

Synthesis. *Synthesis of* ***1a.*** One equivalent of silver nitrate (46 mg, 0.27 mmol) was added to a solution of cisplatin (80 mg, 0.27 mmol) in 10 mL of DMF. The reaction mixture was stirred

overnight at 60 °C. The next day, the AgCl was removed, and one equiv of 1-adamantylamine (41 mg, 0.27 mmol) was added to the filtrate. The reaction mixture was stirred overnight at 60 °C. To the clear reaction mixture, 10 mL of MeOH was added followed by 30 mL of Et_2O. The resulting solution was taken to dryness under vacuum, washed with dichloromethane, and dried, forming the desired product.

1a. Yield: 55 %. ^{1}H NMR (700 MHz, DMSO-d_6): δ = 1.52 (d, 3H, CH_{eq}), 1.61 (d, 3H, CH_{ax}), 1.80 (s, 6H, CH_2), 2.01 (s, 3H, CH), 3.9 (bs, 3H, NH_3), 4.2 (bs, 3H, NH_3), 4.8 (bs, 2H, NH_2) ppm. ^{13}C NMR (125 MHz, DMF-d_7): δ = 29.8 (C10-C12), 36.2 (C13-C15), 43.7 (C7-C9), 54.8 (C6) ppm. ^{195}Pt NMR (DMF-d_7): δ = –2406 ppm. ESI-MS(+) m/z 416.1220, calcd. 416.1214.

*Synthesis of cis-Aqua complex **1a_aq**.* $AgNO_3$ (0.024 mmol, 4 mg) was added to a solution of **1a** (0.024 mmol, 10 mg) in 5 mL of D_2O. The reaction mixture was stirred in the dark at 60°C for 24 h, and the precipitated AgCl was filtered off. The filtrate contains the aqua form **1a_aq**, where chloride has been replaced by water. The filtrate was used for ^{195}Pt and ^{1}H NMR measurements without further purification.

1a_aq. ^{1}H-NMR (700 MHz, D_2O): δ = 1.57 (d, 3H, CH_{eq}), 1.64 (d, 3H, CH_{ax}), 1.80 (s, 6H, CH_2), 2.05 (s, 3H, CH) ppm. ^{195}Pt NMR (D_2O): δ = –2140 ppm

*Synthesis of **2a**.* To a solution of transplatin (0.33 mmol, 100 mg) in 7 mL of DMF, $AgNO_3$ (0.33 mmol, 56 mg) was added. The reaction mixture was stirred in the dark at 55°C for 16 h, and the precipitated AgCl was filtered off. Then 0.9 equiv of 1-adamantylamine (0.30 mmol, 44 mg) was added to the supernatant, and the reaction was stirred for an additional 24 h at 55°C. To the clear reaction mixture, 10 mL of MeOH was added, followed by 30 mL of Et_2O to obtain the product. The white product was precipitated, filtered, and washed with additional Et_2O (3 x 10 mL).

2a. Yield: 50 %. ^{1}H NMR (700 MHz, DMSO-d_6): δ = 1.55 (d, 3H, CH_{eq}), 1.64 (d, 3H, CH_{ax}), 1.75 (s, 6H, CH_2), 2.04 (s, 3H, CH), 3.9 (bs, 6H, NH_3), 5.3 (bs, 2H, NH_2) ppm. ^{13}C NMR (125 MHz, DMF-d_7): δ = 29.2 (C10-C12), 36.1 (C13-C15), 43.6 (C7-C9), 55.5 (C6) ppm. ^{195}Pt NMR (DMF-d_7): δ = –2430 ppm. ESI-MS(+) m/z 416.1212, calcd. 416.1214.

Synthesis of trans-Aqua Complex ***2a_aq.*** $AgNO_3$ (0.024 mmol, 4 mg) was added to a solution of **2a** (0.024 mmol, 10 mg) in 5 mL D_2O. The reaction mixture was stirred in the dark at 60°C for 24 h, and the precipitated AgCl was filtered off. The filtrate containing **2a_aq** was used for ^{195}Pt and ^{1}H NMR measurements without further purification.

2a_aq. ^{1}H-NMR (700 MHz, D_2O): δ = 1.55 (d, 3H, CH_{eq}), 1.62 (d, 3H, CH_{ax}), 1.77 (s, 6H, CH_2), 2.04 (s, 3H, CH) ppm. ^{195}Pt NMR (D_2O): δ = –2177 ppm.

Synthesis of ***3a****.* $PtCl_2$ (0.37 mmol, 100 mg) was suspended in 5 mL of DMF. To the suspension, two equiv of 1-adamantylamine (0.74 mmol, 112 mg) was added. The reaction mixture was refluxed at 100°C for 24 h. A yellow solution was obtained, to which 20 mL of diethyl ether was added, and the mixture was left to evaporate overnight. After that, the product crystallized and the microcrystals were filtered off and washed with diethyl ether.

3a*.* Yield: 50 %. ^{1}H NMR (700 MHz, DMSO-d_6): δ = 1.52 (d, 3H, CH_{eq}), 1.60 (d, 3H, CH_{ax}), 1.90 (s, 6H CH_2), 2.01 (s, 3H CH), 4.18 (bs, 2H, NH_2) ppm. ^{13}C NMR (125 MHz, DMF-d_7): δ = 29.7 (C10-C12), 36.3 (C13-C15), 44.4 (C7-C9), 54.8 (C6) ppm. ^{195}Pt NMR (DMF-d_7): δ = –2179 ppm. ESI-MS(–) m/z 452.0052, calcd. 452.0056.

Synthesis of ***4a****.* K_2PtCl_4 (0.25 mmol, 103 mg) was suspended in 2 mL of DMF. To the suspension an excess amount of 1-adamantylamine (1 mmol, 152 mg) was added. The mixture was stirred at 100°C for 24 h. After that, a white precipitate formed in the solution. The product was filtered off and washed several times with small portions of cold water and diethyl ether.

4a. Yield: 50 %. ^{1}H NMR (700 MHz, DMSO-d_6): δ = 1.51 (d, 3H, CH_{eq}), 1.58 (d, 3H, CH_{ax}), 1.89 (s, 6H, CH_2), 2.00 (s, 3H, CH), 4.20 (bs, 2H, NH_2) ppm. ^{13}C NMR (125 MHz, DMF-d_7): δ = 29.9 (C10-C12), 36.3 (C13-C15), 44.4 (C7-C9), 54.8 (C6) ppm. ^{195}Pt NMR (DMF-d_7): δ = –2180 ppm. ESI-MS(–) m/z 603.1417 $[M+Cl]^-$ calcd. 603.1421.

Synthesis of ***5a, 5b,*** *and* ***5c.*** Potassium tetrachloroplatinate(II) (100 mg, 0.24 mmol) was dissolved in DMF. A solution of two equiv of amine in DMF was added. The resultant red mixture was heated at 70 °C for 3 h until the color of the solution changed to yellow. The reaction was completed by stirring overnight at room temperature. The precipitated potassium chloride was removed by filtration. The filtrate was evaporated to dryness. The residue was washed with water, acetone, and ether and dried. The purified product was obtained as a yellowish-white solid. Crystals of **5b** and **5c** suitable for X-ray analysis were obtained by slowly evaporating the solvent from a DMF solution.

5a. Yield: 55 %. ^{1}H NMR (700 MHz, DMF-d_7): δ = 1.56 – 1.79 (dd), 2.08 (s), 2.26 (m) ppm. ^{13}C NMR (125 MHz, DMF-d_7): δ = 29.8 (C10-C12), 35.9 (C13-C15), 45.1 (C7-C9), 56.0 (C6) ppm. ^{195}Pt NMR (DMF-d_7): δ = –2174 ppm. IR (cm^{-1}): 3223 m (N–H), 2899 m (C–H), 1573 m (N–H). ESI-MS: m/z 603.1425 $[M+Cl]^-$ calcd. 603.1421. **5b**: Yield: 55 %. ^{1}H NMR (700 MHz, DMF-d_7): δ = 1.80 – 2.20 (m), 2.40 (s), 5.60 (bs, 4H, NH_2) ppm. ^{195}Pt NMR (DMF-d_7): δ = –2229 ppm. IR (cm^{-1}): 3223 m (N–H), 2899 m (C–H), 1573 m (N–H). ESI-MS: m/z 659.2047 $[M+Cl]^-$ calcd. 659.2073. **5c**: Yield: 43 %. ^{1}H NMR (700 MHz, DMF-d_7): δ = 1.30 (s), 1.35 – 1.40 (m), 1.5 (s), 1.55 – 1.60 (m), 1.70 – 2.10 (m), 5.80 (bs, 4H, NH_2) ppm. ^{195}Pt NMR (DMF-d_7): δ = –2213 ppm. IR (cm^{-1}): 3203 m (N–H), 2950, 2881 m (C–H), 1667 m (N–H). ESI-MS(+) m/z 595.1953 $[M+Na]^+$ calcd. 595.1908, ESI-MS(–) m/z 607.1710 $[M+Cl]^-$ calcd. 607.1699.

Synthesis of ***6b*** *and* ***6c****. cis*-Diamminediiodoplatinum(II) (60 mg, 0.12 mmol) was suspended in DMF and silver nitrate (41 mg, 0.24 mmol) was added. The suspension was stirred in the dark

at room temperature overnight. The precipitated silver iodide was removed by filtration. Two equivalents of amine were added to the filtrate, and the suspension was heated to 70°C for 3 h. The reaction mixture was cooled to room temperature and filtered, and the filtrate was evaporated to dryness under reduced pressure. The residue was dissolved in 240 µL of 35% hydrochloric acid. The mixture was refluxed for 2 h, 400 µL of distilled water was added, and the heating was continued for another 3 h. The yellow product was suspended in 3 mL of distilled water, stirred for 30 min, and filtered. The filtrate was cooled in a refrigerator, and after 1 week, a second portion of the product was collected. The yellow precipitate was dried.

6b. Yield: 33 %. ^{1}H NMR (700 MHz, DMF-d_7): δ = 1.3 (d), 1.6 – 1.8 (m), 1.9 – 2.0 (m), 2.0 (s), 2.3 – 2.4 (m), 2.5 (s), 5.7 (bs, 3H, NH_3), 6.3 (bs, 2H, NH_2) ppm. ^{195}Pt NMR (DMF-d_7): δ = –2158 ppm. IR (cm^{-1}): 3159 m (N–H), 2952 m (C–H), 1658 m (N–H). ESI-MS(–) m/z 497.0638 $[M+Cl]^-$ calcd. 497.0635 m/z 514.0910 $[M+NH_3+Cl]^-$ calcd. 514.0869. **6c**: Yield: 38 %, ^{1}H NMR (DMF-d_7): δ = 1.7 (d, 3H, CH_3), 2.0 (s, 6H, CH_2), 2.0 – 2.2 (m, 6H, CH_2), 2.3 (s, 3H, CH), 2.4 (s, 1H, CH), 5.7 (bs, 3H, NH_3), 6.1 (bs, 2H, NH_2) ppm. ^{195}Pt NMR (DMF-d_7): δ = –2166 ppm. IR (cm^{-1}): 3419, 3158 m (N–H), 2899, 2848 m (C–H), 1655 m (N–H); ESI-MS(+) m/z 454.1153 $[M+H_2O]^+$ calcd. 454.0865.

*Synthesis of **7d**.* A solution of 1-azabicyclo[2.2.2]octane (ABCO) (28 mg, 0.24 mmol) in 2 mL of methanol was added to a solution of K_2PtCl_4 (50 mg, 0.12 mmol) in 5 mL of deionized water, and the reaction mixture was stirred at room temperature overnight leading to the formation of the product as a yellow precipitate. The product was filtered off the reaction mixture, washed with cold ethanol (1 mL) and diethyl ether (2 mL), and dried under a vacuum. Yellow crystals of the product were grown by slowly evaporating the solvent from a solution of the Pt-complex in chloroform.

7d. Yield 20 mg (32%), mp >208°C dec; ^{1}H NMR (500 MHz, $CDCl_3$) δ = 1.64 (td, *J* = 7.8 Hz, *J* = 3.2 Hz, 6H, H9-11), 1.77 (hept, *J* = 3.2 Hz, 1H, H12), 1.94 (td, *J* = 8.0 Hz, *J* = 3.2 Hz, 6H, H59-61), 2.23 (hept, *J* = 3.2 Hz, 1H, H62), 3.43 (t, *J* = 8.0 Hz, 6H, cation H56-58), 3.55 (t, *J* = 7.8 Hz, 6H, H6-8), 8.93 (br s, 1H, H52) ppm. ^{13}C NMR (125 MHz, $CDCl_3$) δ = 55.6 (C6-C8), 47.3 (C56-C58), 27.0 (C9-C11), 23.2 (C59-C61), 20.3 (C12), 19.9 (C62) ppm. ^{195}Pt ($CDCl_3$): δ = –1782 ppm. ESI-MS(–) m/z 411.9744, calcd. 411.9742.

Synthesis of ***1a@CB7, 1a@β-CD****, and* ***2a@CB7.*** The starting compound (**1a** or **2a**) was complexed with CB7 or *β*-CD in D_2O in a 1 : 1 molar ratio. In procedure for CB7: 9 mg of CB7 was dissolved in a vial, and then 3 mg of the compound was added. The initial mixture was not clear due to the low solubility of the complex in water, but the solution cleared over time as the complex was encapsulated in the macrocycle. Note that the compounds were prepared in situ to perform experiments and analysis.

Evaluation of Biological Activity

Chemical and Biochemical Reagents. RPMI-1640 medium, fetal bovine serum (FBS) (mycoplasma-free), penicillin-streptomycin, and trypsin were purchased from Sigma-Aldrich Co. (St. Louis, MO). Phosphate-buffered saline (PBS) was purchased from Invitrogen Corp. (Carlsbad, CA). Ethylenediaminetetraacetic acid (EDTA), dimethyl sulfoxide (DMSO), and all other chemicals of ACS purity were purchased from Sigma-Aldrich Co., unless noted otherwise.

Cell Lines and Cell Cultivation. Two human ovarian cancer cell lines were used in this study. The A2780 is a human ovarian cancer cell line established from tumor tissue from an untreated patient. The A2780 line is commonly used as a model for monitoring the effects and testing the effectiveness of various chemicals. The A2780/CP cell line was developed by chronic exposure

of the parent cell line to cisplatin. Both cell cultures used in this study were purchased from HPA Culture Collections (Salisbury, U.K.). A2780 and its cisplatin-resistant A2780/CP cell line were cultivated in RPMI-1640 medium with 10% FBS. The cell culture medium was supplemented with antibiotics (penicillin 100 units/mL and streptomycin 0.1 mg/mL). The cells were grown in an incubator (Sanyo) at 37 °C in a humidified 5% CO_2 mixture with ambient air.

Measurement of Cell Viability. The cytotoxicity of our compounds was determined by the MTT assay. The cells were seeded on a 96-well plate at a density of 7×10^3 cells/well in RPMI-1640 medium, containing 10% FBS and 1% penicillin streptomycin and incubated at 37 °C in a humidified 5% CO_2 mixture. After 48 h, the cell culture medium was removed and replaced with a new medium containing cisplatin, cisPt@CB7, cisPt@β-CD, **1a**, **1a@CB7**, or **1a@*β*-CD**. The concentrations of Pt complexes ranged from 0 to 600 μM. After the cells were incubated for 24 or 48 h, 200 μL of medium containing 1 mg/mL MTT agent per well was added. Plates were kept in a humidified atmosphere at 37 °C for 4 h, wrapped in aluminum foil. Then, the medium containing MTT was exchanged with 200 μL of 99.9% DMSO per well to dissolve formazan crystals. The absorbance was read at a wavelength of 570 nm using a Cytation 3 Imaging multimode imaging reader (BioTek Instruments, Winooski, VT). The IC_{50} values are reported as the concentration required to inhibit cell growth by 50%. All measurements were performed in quadruplicate.

Determination of the Pt Content in the Cell Material. Both cell lines were seeded on cell culture dishes (25 cm^2) in RPMI-1640 culture medium, containing 10% FBS and 1% penicillin-streptomycin, and incubated for 24 and 48 h. The cells were then treated with 3.5 μM cisplatin, cisPt@CB7, cisPt@β-CD, **1a**, **1a@CB7**, or **1a@*β*-CD**, each at a sub-IC_{50} concentration. This concentration was applied to detect the accumulation of platinum without inducing extensive cell death. After further incubation for 24 and 48 h, the cells were harvested by trypsinization. The cell samples were washed three times with PBS followed by centrifugation

(4 °C, 2700 rpm, 7 min) to remove the surface-bound drugs. After that, cells were mechanically lysed in PBS on ice with a micropestle for 5 min followed by centrifugation (4 °C, 2700 rpm, 7 min). The platinum concentration of the supernatant collected after the centrifugation was analyzed with an ICP-MS Agilent 7900 (Agilent Technologies). Prepared lysates were diluted 10-fold with Milli-Q water before analysis, and the Pt concentration was measured by using the isotope ^{195}Pt. The quantification was done by external calibration in a range from 0.01 to 10 µg/L of Pt. Possible matrix effects and instability of the plasma conditions were suppressed by an internal standard (a solution of Au with a concentration of 1 µg/L). The amount of platinum was expressed in µg/L and then converted to micrograms of Pt per 10^9 cells.

ASSOCIATED CONTENT

Supporting Information

The Supporting Information is available free of charge at https://pubs.acs.org/doi/10.1021/acs.inorgchem.1c02467. Additional experimental and computational data, additional figures, and Cartesian coordinates (PDF)

Accession Codes

CCDC 2100921-2100924 and 2100928 contains the supplementary crystallographic data for this paper. These data can be obtained free of charge via http://www.ccdc.cam.ac.uk/data_request/cif, or by emailing data_request@ccdc.cam.ac.uk, or by contacting The Cambridge Crystallographic Data Centre, 12 Union Road, Cambridge CB2 1EZ, UK; fax: +44 1223-336-033.

AUTHOR INFORMATION

Corresponding Author

Radek Marek

CEITEC – Central European Institute of Technology, Masaryk University, Kamenice 5, CZ-625 00 Brno, Czechia

Department of Chemistry, Faculty of Science, Masaryk University, Kamenice 5, CZ-625 00 Brno, Czechia

* E-mail: rmarek@chemi.muni.cz

Authors

Martin Sojka

CEITEC – Central European Institute of Technology, Masaryk University, Kamenice 5, CZ-625 00 Brno, Czechia

Department of Chemistry, Faculty of Science, Masaryk University, Kamenice 5, CZ-625 00 Brno, Czechia

Jan Chyba

CEITEC – Central European Institute of Technology, Masaryk University, Kamenice 5, CZ-625 00 Brno, Czechia

Department of Chemistry, Faculty of Science, Masaryk University, Kamenice 5, CZ-625 00 Brno, Czechia

Shib S. Paul

CEITEC – Central European Institute of Technology, Masaryk University, Kamenice 5, CZ-625 00 Brno, Czechia

Department of Chemistry, Faculty of Science, Masaryk University, Kamenice 5, CZ-625 00 Brno, Czechia

Karolina Wawrocka

CEITEC – Central European Institute of Technology, Masaryk University, Kamenice 5, CZ-625 00 Brno, Czechia

Department of Chemistry, Faculty of Science, Masaryk University, Kamenice 5, CZ-625 00 Brno, Czechia

Kateřina Hönigová

Department of Pathological Physiology, Faculty of Medicine, Masaryk University, Kamenice 5, CZ-62500 Brno, Czechia

Ben J. R. Cuyacot

CEITEC – Central European Institute of Technology, Masaryk University, Kamenice 5, CZ-625 00 Brno, Czechia

Department of Chemistry, Faculty of Science, Masaryk University, Kamenice 5, CZ-625 00 Brno, Czechia

Abril C. Castro

Hylleraas Centre for Quantum Molecular Sciences, Department of Chemistry, University of Oslo, P.O. Box 1033 Blindern, 0315 Oslo, Norway

Tomáš Vaculovič

Department of Chemistry, Faculty of Science, Masaryk University, Kamenice 5, CZ-625 00 Brno, Czechia

Jaromír Marek

CEITEC – Central European Institute of Technology, Masaryk University, Kamenice 5, CZ-625 00 Brno, Czechia

Michal Repisky

Hylleraas Centre for Quantum Molecular Sciences, Department of Chemistry, UiT – The Arctic University of Norway, 9037 Tromsø, Norway

Michal Masařík

Department of Pathological Physiology, Faculty of Medicine, Masaryk University, Kamenice 5, CZ-62500 Brno, Czechia

Department of Physiology, Faculty of Medicine, Masaryk University, Kamenice 5, CZ-62500 Brno, Czechia

Jan Novotný

CEITEC – Central European Institute of Technology, Masaryk University, Kamenice 5, CZ-625 00 Brno, Czechia

Department of Chemistry, Faculty of Science, Masaryk University, Kamenice 5, CZ-625 00 Brno, Czechia

Notes

The authors declare no competing financial interest. The computational results are available in the ioChem-BD repository[99] and can be accessed via 10.19061/iochem-bd-6-98.

ACKNOWLEDGMENTS

This work has received support from the Czech Science Foundation (Grant Nos. 21-06991S and 16-05961S to R.M.), the Ministry of Education, Youth and Sports of the Czech Republic (Grant No. 8JPL19045), and the Masaryk University Foundation (Grant Nos. MUNI/A/1390/2020 and MUNI/A/1698/2020). CIISB, Instruct-CZ Center of Instruct-ERIC EU consortium, funded by the MEYS CR Infrastructure Project LM2018127, is gratefully acknowledged for the financial support of the measurements at the Core Facilities Josef Dadok National NMR Center, the CF X-ray diffraction and Bio-SAXS, and MS measurements at the Proteomics Core Facility. The authors thank Dr. Bittova for the ESI-MS measurements at the Department of Chemistry, Faculty of Science, Masaryk University. The computational resources were supported by MEYS CR from the Large Infrastructures for Research, Experimental Development, and Innovations project "e-Infrastructure CZ – LM2018140". A.C.C. and M.R. acknowledge support from the Norwegian Research Council through Grant No. 262695 (CoE Hylleraas Centre for Quantum Molecular Sciences). A.C.C. also acknowledges the European Union's Framework Programme for Research and Innovation Horizon 2020 (2014−2020) under the Marie Skłodowska-Curie Grant Agreement 794563 (ReaDy-NMR).

REFFERENCES

(1) Metal-Based Anticancer Agents. *In Metallobiology*; Casini, A., Vessières, A., Meier-Menches, S. M., Eds.; Metallobiology; Royal Society of Chemistry: Cambridge, 2019. DOI: 10.1039/9781788016452.

(2) Johnstone, T. C.; Suntharalingam, K.; Lippard, S. J. The Next Generation of Platinum Drugs: Targeted Pt(II) Agents, Nanoparticle Delivery, and Pt(IV) Prodrugs. *Chem. Rev.* **2016**, *116* (5), 3436–3486.

(3) Anthony, E. J.; Bolitho, E. M.; Bridgewater, H. E.; Carter, O. W. L.; Donnelly, J. M.; Imberti, C.; Lant, E. C.; Lermyte, F.; Needham, R. J.; Palau, M.; Sadler, P. J.; Shi, H.; Wang, F.-X.; Zhang, W.-Y.; Zhang, Z. Metallodrugs Are Unique: Opportunities and Challenges of Discovery and Development. *Chem. Sci.* **2020**, *11* (48), 12888–12917.

(4) Abu-Surrah, A.; Kettunen, M. Platinum Group Antitumor Chemistry: Design and Development of New Anticancer Drugs Complementary to Cisplatin. *Curr. Med. Chem.* **2006**, *13* (11), 1337–1357.

(5) Brabec, V.; Hrabina, O.; Kasparkova, J. Cytotoxic Platinum Coordination Compounds. DNA Binding Agents. *Coord. Chem. Rev.* **2017**, *351*, 2–31.

(6) Harper, B. W.; Krause-Heuer, A. M.; Grant, M. P.; Manohar, M.; Garbutcheon-Singh, K. B.; Aldrich-Wright, J. R. Advances in Platinum Chemotherapeutics. *Chem. - Eur. J.* **2010**, *16* (24), 7064–7077.

(7) *Bioinorganic Medicinal Chemistry*; Alessio, E., Ed.; Wiley-VCH Verlag GmbH & Co. KGaA: Weinheim, Germany, 2011. DOI: 10.1002/9783527633104.

(8) Li, W.; Jiang, M.; Cao, Y.; Yan, L.; Qi, R.; Li, Y.; Jing, X. Turning Ineffective Transplatin into a Highly Potent Anticancer Drug via a Prodrug Strategy for Drug

Delivery and Inhibiting Cisplatin Drug Resistance. *Bioconjug. Chem.* **2016**, *27* (8), 1802–1806.

(9) Rochon, F. D.; Doyon, M.; Butler, I. S. Synthesis and Characterization of Platinum(II) Complexes with Adamantanamine Derivatives and Related Ligands. *Inorg. Chem.* **1993**, *32* (12), 2717–2723.

(10) Braddock, P. D.; Connors, T. A.; Jones, M.; Khokhar, A. R.; Melzack, D. H.; Tobe, M. L. Structure and Activity Relationships of Platinum Complexes with Anti-Tumour Activity. *Chem. Biol. Interact.* **1975**, *11* (3), 145–161.

(11) Lu, C.; Perez-Soler, R.; Piperdi, B.; Walsh, G. L.; Swisher, S. G.; Smythe, W. R.; Shin, H. J.; Ro, J. Y.; Feng, L.; Truong, M.; Yalamanchili, A.; Lopez-Berestein, G.; Hong, W. K.; Khokhar, A. R.; Shin, D. M. Phase II Study of a Liposome-Entrapped Cisplatin Analog (L-NDDP) Administered Intrapleurally and Pathologic Response Rates in Patients With Malignant Pleural Mesothelioma. *J. Clin. Oncol.* **2005**, *23* (15), 3495–3501.

(12) Jun, Y. J.; Kim, J. I.; Jun, M. J.; Sohn, Y. S. Selective Tumor Targeting by Enhanced Permeability and Retention Effect. Synthesis and Antitumor Activity of Polyphosphazene–Platinum (II) Conjugates. *J. Inorg. Biochem.* **2005**, *99* (8), 1593–1601.

(13) Dragovich, T.; Mendelson, D.; Kurtin, S.; Richardson, K.; Von Hoff, D.; Hoos, A. A Phase 2 Trial of the Liposomal DACH Platinum L-NDDP in Patients with Therapy-Refractory Advanced Colorectal Cancer. *Cancer Chemother. Pharmacol.* **2006**, *58* (6), 759–764.

(14) Rice, J. R.; Gerberich, J. L.; Nowotnik, D. P.; Howell, S. B. Preclinical Efficacy and Pharmacokinetics of AP5346, A Novel Diaminocyclohexane-Platinum Tumor-Targeting Drug Delivery System. *Clin. Cancer Res.* **2006**, *12* (7), 2248–2254.

(15) Domínguez, C. S. H.; Hernández, P. Use of Cucurbit [6] Uril as a Modifier in the Electrochemical Determination of Antitumor Platinum (II) Complex: Trans-[$PtCl_2$(Dimethylamine) (Isopropylamine)]. Application to Biological Samples. *Am. J. Anal. Chem.* **2013**, *04* (06), 314–322.

(16) Gao, C.; Fei, F.; Wang, T.; Yang, B.; Gou, S.; Yang, J.; Liao, L. Synthesis and *in Vitro* Cytotoxicity of Platinum(II) Complexes with Chiral N-Monosubstituted 1,2-Cyclohexyldiamine Derivatives as the Carrier Groups. *J. Coord. Chem.* **2013**, *66* (6), 1068–1076.

(17) Komeda, S.; Takayama, H.; Suzuki, T.; Odani, A.; Yamori, T.; Chikuma, M. Synthesis of Antitumor Azolato-Bridged Dinuclear Platinum(II) Complexes with in Vivo Antitumor Efficacy and Unique in Vitro Cytotoxicity Profiles. *Metallomics* **2013**, *5* (5), 461–468.

(18) *Ligand Design in Medicinal Inorganic Chemistry: Storr/Ligand Design in Medicinal Inorganic Chemistry*; Storr, T., Ed.; John Wiley & Sons, Ltd: Chichester, UK, 2014. DOI: 10.1002/9781118697191.

(19) Komeda, S.; Uemura, M.; Yoneyama, H.; Harusawa, S.; Hiramoto, K. In Vitro Cytotoxicity and In Vivo Antitumor Efficacy of Tetrazolato-Bridged Dinuclear Platinum(II) Complexes with a Bulky Substituent at Tetrazole C5. *Inorganics* **2019**, *7* (1), 5.

(20) Wheate, N. J. Improving Platinum(II)-Based Anticancer Drug Delivery Using Cucurbit[n]Urils. *J. Inorg. Biochem.* **2008**, *102* (12), 2060–2066.

(21) Wheate, N. J.; Buck, D. P.; Day, A. I.; Collins, J. G. Cucurbit[n]Uril Binding of Platinum Anticancer Complexes. *Dalton Trans* **2006**, No. 3, 451–458.

(22) Jin Jeon, Y.; Kim, S.-Y.; Ho Ko, Y.; Sakamoto, S.; Yamaguchi, K.; Kim, K. Novel Molecular Drug Carrier: Encapsulation of Oxaliplatin in Cucurbit[7]Uril and Its Effects on Stability and Reactivity of the Drug. *Org. Biomol. Chem.* **2005**, *3* (11), 2122.

(23) Plumb, J. A.; Venugopal, B.; Oun, R.; Gomez-Roman, N.; Kawazoe, Y.; Venkataramanan, N. S.; Wheate, N. J. Cucurbit[7]Uril Encapsulated Cisplatin Overcomes Cisplatin Resistance via a Pharmacokinetic Effect. *Metallomics* **2012**, *4* (6), 561.

(24) Tian, B.; Hua, S.; Liu, J. Cyclodextrin-Based Delivery Systems for Chemotherapeutic Anticancer Drugs: A Review. *Carbohydr. Polym.* **2020**, *232*, 115805.

(25) Wankar, J.; Kotla, N. G.; Gera, S.; Rasala, S.; Pandit, A.; Rochev, Y. A. Recent Advances in Host–Guest Self-Assembled Cyclodextrin Carriers: Implications for Responsive Drug Delivery and Biomedical Engineering. *Adv. Funct. Mater.* **2020**, *30* (44), 1909049.

(26) Uekama, K.; Hirayama, F.; Irie, T. Cyclodextrin Drug Carrier Systems. *Chem. Rev.* **1998**, *98* (5), 2045–2076.

(27) Gu, A.; Wheate, N. J. Macrocycles as Drug-Enhancing Excipients in Pharmaceutical Formulations. *J. Incl. Phenom. Macrocycl. Chem.* **2021**, *100* (1–2), 55–69.

(28) Das, D.; Assaf, K. I.; Nau, W. M. Applications of Cucurbiturils in Medicinal Chemistry and Chemical Biology. *Front. Chem.* **2019**, *7*, 619.

(29) Prashar, D.; Shi, Y.; Bandyopadhyay, D.; Dabrowiak, J. C.; Luk, Y.-Y. Adamantane–Platinum Conjugate Hosted in β-Cyclodextrin: Enhancing Transport and Cytotoxicity by Noncovalent Modification. *Bioorg. Med. Chem. Lett.* **2011**, *21* (24), 7421–7425.

(30) Wanka, L.; Iqbal, K.; Schreiner, P. R. The Lipophilic Bullet Hits the Targets: Medicinal Chemistry of Adamantane Derivatives. *Chem. Rev.* **2013**, *113* (5), 3516–3604.

(31) Webber, M. J.; Langer, R. Drug Delivery by Supramolecular Design. *Chem. Soc. Rev.* **2017**, *46* (21), 6600–6620.

(32) Ma, X.; Zhao, Y. Biomedical Applications of Supramolecular Systems Based on Host–Guest Interactions. *Chem. Rev.* **2015**, *115* (15), 7794–7839.

(33) Sojka, M.; Fojtu, M.; Fialova, J.; Masarik, M.; Necas, M.; Marek, R. Locked and Loaded: Ruthenium(II)-Capped Cucurbit[*n*]Uril-Based Rotaxanes with Antimetastatic Properties. *Inorg. Chem.* **2019**, *58* (16), 10861–10870.

(34) Murray, J.; Kim, K.; Ogoshi, T.; Yao, W.; Gibb, B. C. The Aqueous Supramolecular Chemistry of Cucurbit[n]Urils, Pillar[n]Arenes and Deep-Cavity Cavitands. *Chem. Soc. Rev.* **2017**, *46* (9), 2479–2496.

(35) Geng, W.-C.; Sessler, J. L.; Guo, D.-S. Supramolecular Prodrugs Based on Host–Guest Interactions. *Chem. Soc. Rev.* **2020**, *49* (8), 2303–2315.

(36) Wilson, J. J.; Lippard, S. J. Synthetic Methods for the Preparation of Platinum Anticancer Complexes. *Chem. Rev.* **2014**, *114* (8), 4470–4495.

(37) Ren, T.; Bancroft, D. P.; Sundquist, W. I.; Masschelein, A.; Keck, M. V.; Lippard, S. J. Synthesis, Characterization, DNA Binding Properties, and Solution Thermochromism of Platinum(II) Complexes of the Ethidium Cation: Regiospecificity in a DNA-Promoted Reaction. *J. Am. Chem. Soc.* **1993**, *115* (24), 11341–11352.

(38) Rochon, F. D.; Tessier, C. *Cis* -Bis[(1-Adamantylmethyl)Amine-κ *N*]Dichloridoplatinum(II) *N*,*N*-Dimethylformamide Solvate. *Acta Crystallogr. Sect. E Struct. Rep. Online* **2009**, *65* (11), m1297–m1298.

(39) Mareque Rivas, J. C.; Brammer, L. Self-Assembly of 1-D Chains of Different Topologies Using the Hydrogen-Bonded Inorganic Supramolecular Synthons N−H···Cl $_2$ M or N−H···Cl $_3$ M. *Inorg. Chem.* **1998**, *37* (19), 4756–4757.

(40) Cromwell, W. C.; Bystrom, K.; Eftink, M. R. Cyclodextrin-Adamantanecarboxylate Inclusion Complexes: Studies of the Variation in Cavity Size. *J. Phys. Chem.* **1985**, *89* (2), 326–332.

(41) Baykal, A.; Bozkurt, A.; Jeremy, R.; Asiri, S. M. M.; Lima-Tenório, M. K.; Kaewsaneha, C.; Elaissari, A. Multistimuli-Responsive Magnetic Assemblies. In *Stimuli Responsive Polymeric Nanocarriers for Drug Delivery Applications*; Elsevier, 2019; pp 155–193. DOI: 10.1016/B978-0-08-101995-5.00006-4.

(42) Assaf, K. I.; Nau, W. M. Cucurbiturils: From Synthesis to High-Affinity Binding and Catalysis. *Chem. Soc. Rev.* **2015**, *44* (2), 394–418.

(43) Kolman, V.; Marek, R.; Strelcova, Z.; Kulhanek, P.; Necas, M.; Svec, J.; Sindelar, V. Electron Density Shift in Imidazolium Derivatives upon Complexation with Cucurbit[6]Uril. *Chem. - Eur. J.* **2009**, *15* (28), 6926–6931.

(44) Kolman, V.; Babinský, M.; Kulhánek, P.; Marek, R.; Sindelar, V. Redistribution of Electron Density in Pyridinium and Pyrazinium Guests Induced by Complexation with Cucurbit[6]Uril. *New J. Chem.* **2011**, *35* (12), 2854-2859.

(45) Bora, P. L.; Novák, M.; Novotný, J.; Foroutan-Nejad, C.; Marek, R. Supramolecular Covalence in Bifurcated Chalcogen Bonding. *Chem. - Eur. J.* **2017**, *23* (30), 7315–7323.

(46) Branná, P.; Černochová, J.; Rouchal, M.; Kulhánek, P.; Babinský, M.; Marek, R.; Nečas, M.; Kuřitka, I.; Vícha, R. Cooperative Binding of Cucurbit[n]Urils and β-Cyclodextrin to Heteroditopic Imidazolium-Based Guests. *J. Org. Chem.* **2016**, *81* (20), 9595–9604.

(47) Chyba, J.; Novák, M.; Munzarová, P.; Novotný, J.; Marek, R. Through-Space Paramagnetic NMR Effects in Host–Guest Complexes: Potential Ruthenium(III) Metallodrugs with Macrocyclic Carriers. *Inorg. Chem.* **2018**, *57* (15), 8735–8747.

(48) Malali, S.; Chyba, J.; Knor, M.; Horní, M.; Nečas, M.; Novotný, J.; Marek, R. Zwitterionic Ru(III) Complexes: Stability of Metal–Ligand Bond and Host–Guest Binding with Cucurbit[7]Uril. *Inorg. Chem.* **2020**, *59* (14), 10185–10196.

(49) Bancroft, D. P.; Lepre, C. A.; Lippard, S. J. Platinum-195 NMR Kinetic and Mechanistic Studies of Cis- and Trans-Diamminedichloroplatinum(II) Binding to DNA. *J. Am. Chem. Soc.* **1990**, *112* (19), 6860–6871.

(50) Kozelka, J. Hydrolysis of Chlorido Complexes of D8 Metals: Old Models, New Facts. *Inorganica Chim. Acta* **2019**, *495*, 118946.

(51) Zhang, Y.; Guo, Z.; You, X.-Z. Hydrolysis Theory for Cisplatin and Its Analogues Based on Density Functional Studies. *J. Am. Chem. Soc.* **2001**, *123* (38), 9378–9387.

(52) Velde, G. T.; Bickelhaupt, F. M.; Baerends, E. J.; Guerra, C. F.; Gisbergen, S. J. A. V. Chemistry with ADF. *J. Comput. Chem.* **2001**, *22*, 2001.

(53) Repisky, M.; Komorovsky, S.; Kadek, M.; Konecny, L.; Ekström, U.; Malkin, E.; Kaupp, M.; Ruud, K.; Malkina, O. L.; Malkin, V. G. ReSpect: Relativistic Spectroscopy DFT Program Package. *J. Chem. Phys.* **2020**, *152* (18), 184101.

(54) van Lenthe, E.; Baerends, E. J.; Snijders, J. G. Relativistic Regular Two-component Hamiltonians. *J. Chem. Phys.* **1993**, *99* (6), 4597–4610.

(55) van Lenthe, E.; Snijders, J. G.; Baerends, E. J. The Zero-order Regular Approximation for Relativistic Effects: The Effect of Spin–Orbit Coupling in Closed Shell Molecules. *J. Chem. Phys.* **1996**, *105* (15), 6505–6516.

(56) Komorovský, S.; Repiský, M.; Malkina, O. L.; Malkin, V. G.; Malkin Ondík, I.; Kaupp, M. A Fully Relativistic Method for Calculation of Nuclear Magnetic Shielding Tensors with a Restricted Magnetically Balanced Basis in the Framework of the Matrix Dirac–Kohn–Sham Equation. *J. Chem. Phys.* **2008**, *128* (10), 104101.

(57) Komorovský, S.; Repiský, M.; Malkina, O. L.; Malkin, V. G. Fully Relativistic Calculations of NMR Shielding Tensors Using Restricted Magnetically Balanced Basis and Gauge Including Atomic Orbitals. *J. Chem. Phys.* **2010**, *132* (15), 154101.

(58) Remigio, R. D.; Repisky, M.; Komorovsky, S.; Hrobarik, P.; Frediani, L.; Ruud, K. Four-Component Relativistic Density Functional Theory with the Polarisable Continuum Model: Application to EPR Parameters and Paramagnetic NMR Shifts. *Mol. Phys.* **2017**, *115* (1–2), 214–227.

(59) Konecny, L.; Kadek, M.; Komorovsky, S.; Ruud, K.; Repisky, M. Resolution-of-Identity Accelerated Relativistic Two- and Four-Component Electron Dynamics Approach to Chiroptical Spectroscopies. *J. Chem. Phys.* **2018**, *149* (20), 204104.

(60) Truflandier, L. A.; Sutter, K.; Autschbach, J. Solvent Effects and Dynamic Averaging of ^{195} Pt NMR Shielding in Cisplatin Derivatives. *Inorg. Chem.* **2011**, *50* (5), 1723–1732.

(61) Fong, C. W. Cisplatin Cyclodextrin Complexes as Potential Free Radical Chemoradiosensitizers for Enhanced Cisplatin Treatment of Cancers: A Quantum Mechanical Study. *J. Incl. Phenom. Macrocycl. Chem.* **2017**, *89* (3–4), 343–351.

(62) Dasari, S.; Tchounwou, B. P. Cisplatin in Cancer Therapy: Molecular Mechanisms of Action. *Eur. J. Pharmacol.* **2014**, *740*, 364–378.

(63) Wheate, N. J.; Day, A. I.; Blanch, R. J.; Arnold, A. P.; Cullinane, C.; Grant Collins, J. Multi-Nuclear Platinum Complexes Encapsulated in Cucurbit[n]Uril as an Approach to Reduce Toxicity in Cancer Treatment. *Chem. Commun.* **2004**, No. 12, 1424.

(64) Kemp, S.; Wheate, N. J.; Pisani, M. J.; Aldrich-Wright, J. R. Degradation of Bidentate-Coordinated Platinum(II)-Based DNA Intercalators by Reduced L -Glutathione. *J. Med. Chem.* **2008**, *51* (9), 2787–2794.

(65) Helleman, J.; Burger, H. Impaired Cisplatin Influx in an A2780 Mutant Cell Line: Evidence for a Putative, Cis-Configuration-Specific, Platinum Influx Transporter. *Cancer Biol. Ther.* **2006**, *5* (8), 943–949.

(66) Zisowsky, J.; Koegel, S.; Leyers, S.; Devarakonda, K.; Kassack, M. U.; Osmak, M.; Jaehde, U. Relevance of Drug Uptake and Efflux for Cisplatin Sensitivity of Tumor Cells. *Biochem. Pharmacol.* **2007**, *73* (2), 298–307.

(67) Comsa, E.; Nguyen, K.-A.; Loghin, F.; Boumendjel, A.; Peuchmaur, M.; Andrieu, T.; Falson, P. Ovarian Cancer Cells Cisplatin Sensitization Agents Selected by Mass Cytometry Target ABCC2 Inhibition. *Future Med. Chem.* **2018**, *10* (11), 1349–1360.

(68) Münster, L.; Fojtů, M.; Capáková, Z.; Muchová, M.; Musilová, L.; Vaculovič, T.; Balvan, J.; Kuřitka, I.; Masařík, M.; Vícha, J. Oxidized Polysaccharides for Anticancer-Drug Delivery: What Is the Role of Structure? *Carbohydr. Polym.* **2021**, *257*, 117562.

(69) Hamelers, I. H. L.; Staffhorst, R. W. H. M.; Voortman, J.; de Kruijff, B.; Reedijk, J.; van Bergen en Henegouwen, P. M. P.; de Kroon, A. I. P. M. High Cytotoxicity of Cisplatin Nanocapsules in Ovarian Carcinoma Cells Depends on Uptake by Caveolae-Mediated Endocytosis. *Clin. Cancer Res.* **2009**, *15* (4), 1259–1268.

(70) Vondálová Blanářová, O.; Šafaříková, B.; Herůdková, J.; Krkoška, M.; Tománková, S.; Kahounová, Z.; Anděra, L.; Bouchal, J.; Kharaishvili, G.; Král, M.; Sova, P.; Kozubík, A.; Hyršlová Vaculová, A. Cisplatin or LA-12 Enhance Killing Effects of TRAIL in Prostate Cancer Cells through Bid-Dependent Stimulation of Mitochondrial Apoptotic Pathway but Not Caspase-10. *PLOS ONE* **2017**, *12* (11), e0188584.

(71) Žák, F.; Turánek, J.; Kroutil, A.; Sova, P.; Mistr, A.; Poulová, A.; Mikolin, P.; Žák, Z.; Kašná, A.; Záluská, D.; Neča, J.; Šindlerová, L.; Kozubík, A. Platinum(IV) Complex with Adamantylamine as Nonleaving Amine Group: Synthesis, Characterization, and in Vitro Antitumor Activity against a Panel of Cisplatin-Resistant Cancer Cell Lines. *J. Med. Chem.* **2004**, *47* (3), 761–763.

(72) Bothner-By, A. A.; Stephens, R. L.; Lee, J.; Warren, C. D.; Jeanloz, R. W. Structure Determination of a Tetrasaccharide: Transient Nuclear Overhauser Effects in the Rotating Frame. *J. Am. Chem. Soc.* **1984**, *106* (3), 811–813.

(73) Lee, W.; Tonelli, M.; Markley, J. L. NMRFAM-SPARKY: Enhanced Software for Biomolecular NMR Spectroscopy. *Bioinformatics* **2015**, *31* (8), 1325–1327.

(74) Bodenhausen, G.; Ruben, D. J. Natural Abundance Nitrogen-15 NMR by Enhanced Heteronuclear Spectroscopy. *Chem. Phys. Lett.* **1980**, *69* (1), 185–189.

(75) Sheldrick, G. M. SHELXT – Integrated Space-Group and Crystal-Structure Determination. *Acta Crystallogr. Sect. Found. Adv.* **2015**, *A71* (1), 3–8.

(76) Sheldrick, G. M. Crystal Structure Refinement with SHELXL. *Acta Crystallogr. Sect. C Struct. Chem.* **2015**, *71* (1), 3–8.

(77) Spek, A. L. PLATON SQUEEZE: A Tool for the Calculation of the Disordered Solvent Contribution to the Calculated Structure Factors. *Acta Crystallogr. Sect. C Struct. Chem.* **2015**, *71* (1), 9–18.

(78) Perdew, J. P.; Burke, K.; Ernzerhof, M. Generalized Gradient Approximation Made Simple. *Phys. Rev. Lett.* **1996**, *77* (18), 3865–3868.

(79) Grimme, S. Semiempirical GGA-type density functional constructed with a long-range dispersion correction. *J. Comput. Chem.* **2006**, *27* (15), 1787–1799.

(80) van Lenthe, E.; Baerends, E. J. Optimized Slater-Type Basis Sets for the Elements 1-118. *J. Comput. Chem.* **2003**, *24* (9), 1142–1156.

(81) van Lenthe, E.; Leeuwen, R. van; Baerends, E. J.; Snijders, J. G. Relativistic regular two-component Hamiltonians. *Int. J. Quantum Chem.* **1996**, *57* (3), 281–293.

(82) van Lenthe, E.; Baerends, E. J.; Snijders, J. G. Relativistic Total Energy Using Regular Approximations. *J. Chem. Phys.* **1994**, *101* (11), 9783–9792.

(83) Pye, C. C.; Ziegler, T. An Implementation of the Conductor-like Screening Model of Solvation within the Amsterdam Density Functional Package. *Theor. Chem. Acc.* **1999**, *101* (6), 396–408.

(84) Klamt, A. Calculation of UV/Vis Spectra in Solution. *J. Phys. Chem.* **1996**, *100* (9), 3349–3353.

(85) Klamt, A.; Schüürmann, G. COSMO: A New Approach to Dielectric Screening in Solvents with Explicit Expressions for the Screening Energy and Its Gradient. *J Chem Soc Perkin Trans 2* **1993**, No. 5, 799–805.

(86) Novotný, J.; Vícha, J.; Bora, P. L.; Repisky, M.; Straka, M.; Komorovsky, S.; Marek, R. Linking the Character of the Metal–Ligand Bond to the Ligand NMR Shielding in Transition-Metal Complexes: NMR Contributions from Spin–Orbit Coupling. *J. Chem. Theory Comput.* **2017**, *13* (8), 3586–3601.

(87) Vícha, J.; Novotný, J.; Komorovsky, S.; Straka, M.; Kaupp, M.; Marek, R. Relativistic Heavy-Neighbor-Atom Effects on NMR Shifts: Concepts and Trends Across the Periodic Table. *Chem. Rev.* **2020**, *120* (15), 7065–7103.

(88) Adamo, C.; Barone, V. Toward Reliable Density Functional Methods without Adjustable Parameters: The PBE0 Model. *J. Chem. Phys.* **1999**, *110* (13), 6158–6170.

(89) Dyall, K. G. Relativistic Double-Zeta, Triple-Zeta, and Quadruple-Zeta Basis Sets for the 5d Elements Hf?Hg. *Theor. Chem. Acc.* **2004**, *112* (5–6), 403–409.

(90) Dyall, K. G.; Gomes, A. S. P. Revised Relativistic Basis Sets for the 5d Elements Hf–Hg. *Theor. Chem. Acc.* **2010**, *125* (1–2), 97–100.

(91) Dyall, K. G. Core Correlating Basis Functions for Elements 31–118. *Theor. Chem. Acc.* **2012**, *131* (5), 1217.

(92) Jensen, F. Polarization Consistent Basis Sets: Principles. *J. Chem. Phys.* **2001**, *115* (20), 9113–9125.

(93) Jensen, F. Polarization Consistent Basis Sets. II. Estimating the Kohn–Sham Basis Set Limit. *J. Chem. Phys.* **2002**, *116* (17), 7372–7379.

(94) Fleischer, U.; Kutzelnigg, W.; Limbach, H.-H.; Martin, G. J.; Martin, M. L.; Schindler, M. *Deuterium and Shift Calculation*; Diehl, P., Fluck, E., Günther, H., Kosfeld, R., Seelig, J., Series Eds.; NMR Basic Principles and Progress; Springer Berlin Heidelberg: Berlin, Heidelberg, 1991; Vol. 23. DOI: 10.1007/978-3-642-75932-1.

(95) Stanton, R. E.; Havriliak, S. Kinetic Balance: A Partial Solution to the Problem of Variational Safety in Dirac Calculations. *J. Chem. Phys.* **1984**, *81* (4), 1910–1918.

(96) Ditchfield, R. Self-Consistent Perturbation Theory of Diamagnetism: I. A Gauge-Invariant LCAO Method for N.M.R. Chemical Shifts. *Mol. Phys.* **1974**, *27* (4), 789–807.

(97) Castro, A. C.; Fliegl, H.; Cascella, M.; Helgaker, T.; Repisky, M.; Komorovsky, S.; Medrano, M. Á.; Quiroga, A. G.; Swart, M. Four-Component Relativistic ^{31} P NMR Calculations for *Trans* -Platinum(II) Complexes: Importance of the Solvent and Dynamics in Spectral Simulations. *Dalton Trans.* **2019**, *48* (23), 8076–8083.

(98) Dhara, S. C. A Rapid Method for the Synthesis of Cis-[Pt(NH3)2Cl2]. *Indian J Chem* **1970**, *8* (2), 193–194.

(99) Álvarez-Moreno, M.; de Graaf, C.; López, N.; Maseras, F.; Poblet, J. M.; Bo, C. Managing the Computational Chemistry Big Data Problem: The IoChem-BD Platform. *J. Chem. Inf. Model.* **2015**, *55* (1), 95–103.

TOC graphic

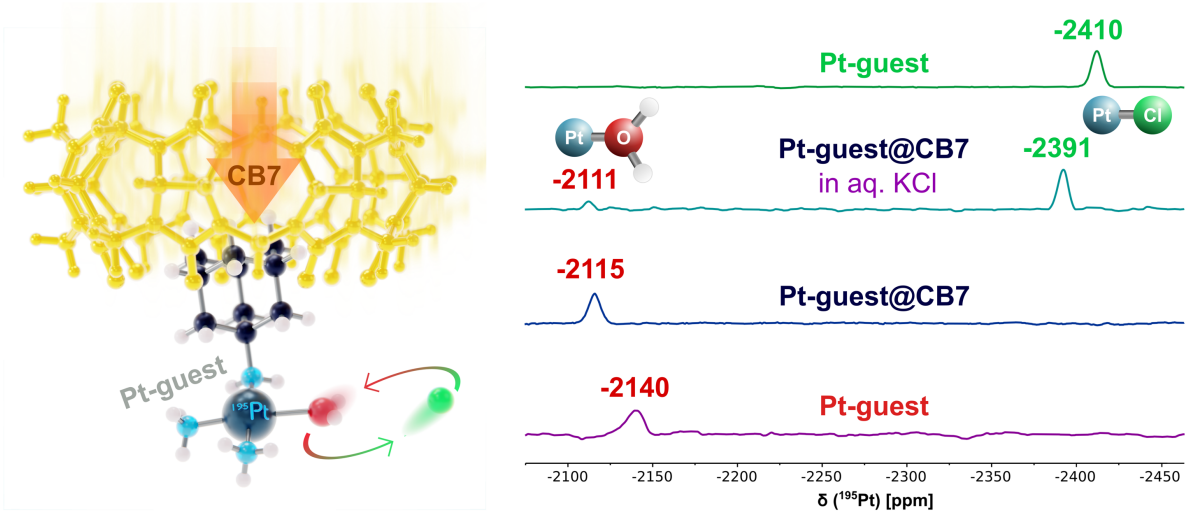

Synopsis

Ionic Pt(II) compounds with bulky anchors were synthesized and bound with macrocyclic cavitands. The hydrolysis of the compounds and host-guest assemblies in aqueous solution was monitored by NMR spectroscopy and showed that the cucurbit[7]uril carrier promoted the aquation of *cis*-[$Pt(NH_3)_2Cl(NH_2$-R)]NO_3. Biological screening of cytotoxicity and platinum uptake by the cells are also reported.